FACULTY OF SCIENCE
PALACKY UNIVERSITY OLOMOUC

Department of Optics

Adaptive operations for entanglement distillation and other applications

DIPLOMA THESIS

Jan Provazník

2017

PŘÍRODOVĚDECKÁ FAKULTA
UNIVERZITA PALACKÉHO V OLOMOUCI

Katedra optiky

Adaptivní operace při destilaci kvantové provázanosti a dalších aplikacích

DIPLOMOVÁ PRÁCE

Jan Provazník

2017

FACULTY OF SCIENCE
PALACKY UNIVERSITY OLOMOUC

Department of Optics

Adaptive operations for entanglement distillation and other applications

DIPLOMA THESIS

Author	Jan Provazník
Study programme	N1701 Physics
Study branch	General Physics and Mathematical Physics
Study form	daily
Supervisor	Mgr. Petr Marek, Ph.D.

PŘÍRODOVĚDECKÁ FAKULTA
UNIVERZITA PALACKÉHO V OLOMOUCI

Katedra optiky

Adaptivní operace při destilaci kvantové provázanosti a dalších aplikacích

DIPLOMOVÁ PRÁCE

Vypracoval	Jan Provazník
Studijní program	N1701 Fyzika
Studijní obor	Obecná fyzika a matematická fyzika
Form studia	prezenční
Vedoucí práce	Mgr. Petr Marek, Ph.D.

Prohlašuji, že jsem diplomovou práci vypracoval samostatně pod dohledem vedoucího práce a za použití uvedených literárních pramenů.

V Olomouci dne 12. 05. 2017

Abstract

Advanced protocols of the contemporary quantum information processing rely on non-Gaussian operations such as the single photon subtraction. The current level of technology permits only conditional realizations of such operations, hindering their usefulness in experimental practice. In this work we focus on improving the success rate of these operations using an iterative approach based on recycling the signal until the conditional operation succeeds. We analyse the properties of the improved subtraction procedure in two distinct scenarios. We apply the operation to superposed coherent states to investigate the preservation of quantum superposition and we employ the improved procedure in a basic quantum entanglement distillation protocol to determine its possible practical impact.

Keywords

quantum optics, continuous variables, Wigner functions, Gaussian states of light, single photon subtraction, adaptive operations, entanglement distillation, coherent cat states

Abstrakt

Pokročilé protokoly soudobého kvantového zpracování informace hojně využívají negausovské operace, jako je například odebrání jednoho fotonu. Současná úroveň techniky umožňuje jen podmíněné realizace takových operací, což znesnadňuje jejich využití v experimentální praxi. V této práci se zabýváme zlepšením pravděpodobnosti úspěchu těchto operací a využíváme iterativního přístupu založeného na recyklaci signálu do té doby, než podmíněná operace uspěje. Vlastnosti takto vylepšené procedury odebrání jednoho fotonu zkoumáme ve dvou odlišných situacích. Aplikací operace na superpozici koherentních stavů ověřujeme zachování kvantových superpozic a konečeně využítím takto vylepšené operace v základním protokolu destilace kvantové provázanosti zkoumáme její možné praktické dopady.

Klíčová slova

kvantová optika, spojité proměnné, Wignerovy funkce, Gausovské stavy světla, odebrání jednoho fotonu, adaptivní operace, destilace kvantové provázanosti, koherentní kočičí stavy

Acknowledgements

First and foremost, I would like to express my gratitude to my supervisor Mgr. Petr Marek, Ph.D. for his kind support, never ending guidance and his seemingly infinite patience with my shenanigans. On a similar note I would like to thank my parents for their financial and emotional support of my endeavours. I would also like to thank one of my cats for always jumping on the keyboard and typing a better half of the document but alas, in some undecipherable dialect.

At last but not least I would like to express my gratitude to everyone who listened to my endless rants and helped me collect my thoughts.

Contents

List of Figures

Introduction

Over the past few decades quantum optics witnessed a rapid development and secured a well deserved position in many areas of the contemporary theoretical, experimental, and applied research, including but not limited to quantum information theory, quantum communications, and quantum cryptography [1, 2, 3].

One of the most appealing aspects of light is its relative resilience to decoherence. However, the very same property is one of its greatest weaknesses as it renders most physical interactions nearly impossible. As a consequence, fields of light in contemporary experiments may usually be manipulated only with linear optical elements constituting a subset of the class of Gaussian operations.

The quantum optical realizations of various concepts of the continuous variable information theory and quantum cryptography employ Gaussian states and consequently rely on Gaussian operations, i.e., elements of linear optics and squeezing. Unfortunately such states and operations are not applicable in some of the more advanced concepts of quantum information theory, e.g., universal quantum computation and quantum entanglement distillation [4, 5, 6, 7, 8, 9, 10]. It was shown that using only Gaussian states and Gaussian operations leaves no room for improvement in entanglement distillation strategies [8, 9, 10]. Similarly universal quantum computation requires at least cubic non-linear interactions [4, 5, 6].

A lot of effort was therefore devoted to circumventing these limitations. Methods based on projective measurements on number states [11], single photon addition [12], and single photon subtraction [12, 13, 14] were successfully implemented, yielding strongly non-Gaussian states of light. Methods based on non-Gaussian operations were devised for entanglement distillation as well, one in particular making use of single photon subtraction [15]. The method was subsequently implemented in experimental setting [16, 17, 18].

In our previous work [19] we focused our attention on the single photon subtraction [13, 14] which was originally presented as a "degaussification" protocol, i.e., a feasible approach to generating non-Gaussian states from pulses of squeezed light.

We proposed an improved version of the subtraction procedure with the intention of enhancing its success rate along with improving its general performance. We analysed the effects of the improved procedure on squeezed vacuum states and consequently demonstrated a significant improvement of performance and a considerable increase in success probability compared to the original subtraction procedure.

In this work we extend our analysis to include a broader variety of scenarios. Firstly we apply the subtraction procedure to superposed coherent states in order to determine how well the procedure conserves superpositions of pure states. Secondly we analyse an adaptation of a basic entanglement distillation protocol [15] employing the improved subtraction procedure on two mode squeezed vacuum states.

This document comprises five chapters. In the first chapter we introduce the mathematical formalism of continuous variable quantum optics and give a brief overview of Gaussian states and operations used in later chapters. In the second chapter we review the original and the improved subtraction procedures, and in the third chapter we develop a suitable mathematical description. The preservation of superposition is analysed using coherent cat states in the fourth chapter. The quantum entanglement distillation procedure is analysed in the fifth chapter and finally we close with a conclusion and outlooks, followed by a pair of appendices providing detailed derivations of mathematical formulae used in the fifth chapter.

Chapter I

Theoretical framework

A pair of distinct approaches is traditionally used in the quantum information theory. The first technique exploits observables of discrete spectra such as polarization states of single photons or excitation levels of individual atoms to encode information in a digital manner. The second technique takes advantage of observables with continuous spectra instead, including generalised position and momentum describing oscillatory behaviour of electromagnetic waves.

The latter approach is commonly referred to as the quantum information theory with continuous variables [4, 5, 6, 20, 21].

1 Continuous variables

An arbitrary quantum physical system is called a continuous variable system if the dimension of the associated Hilbert state space is infinite [5, 6, 22].

A typical continuous variable system common in quantum optics is the quantised electromagnetic field, which can be modelled as a collection of non-interacting harmonic oscillators with different oscillation frequencies and polarizations [22, 23]. Each individual oscillator is usually referred to as a **mode** of the field [4, 5, 22, 23].

The mathematical structure of a single mode of the photonic field is identical to the structure of a one dimensional harmonic oscillator [23, 24] and may be described

using a pair of field operators satisfying the bosonic commutation relation

$$[\hat{a}, \hat{a}^\dagger] = 1 \ . \tag{I.1}$$

The product of the field excitation creation $\hat{a}^\dagger$ and annihilation $\hat{a}$ operators makes up the number operator

$$\hat{n} = \hat{a}^\dagger \hat{a}, \tag{I.2}$$

which is used to define the number basis. The field operators lead to the generalised quadrature operators

$$\hat{x} = \frac{\hat{a} + \hat{a}^\dagger}{\sqrt{2}} \ , \quad \imath\hat{p} = \frac{\hat{a} - \hat{a}^\dagger}{\sqrt{2}} \tag{I.3}$$

satisfying the commutation relation

$$[\hat{x}, \hat{p}] = \imath \ . \tag{I.4}$$

Multiple modes of the photon field are described in the very same fashion, each mode characterized with a unique pair of field operators $\hat{a}_f$ and $\hat{a}_f^\dagger$ acting on the mode [22, 23]. The field operators then satisfy the commutation relations

$$\begin{aligned} [\hat{a}_f, \hat{a}_{f'}^\dagger] &= \delta_{ff'} \\ [\hat{a}_f, \hat{a}_{f'}] = [\hat{a}_f^\dagger, \hat{a}_{f'}^\dagger] &= 0 \end{aligned} \quad \forall \ f, f' \ . \tag{I.5}$$

The quadrature operators related to each mode are defined similarly as

$$\hat{x}_f = \frac{\hat{a}_f + \hat{a}_f^\dagger}{\sqrt{2}} \ , \quad \imath\hat{p}_f = \frac{\hat{a}_f - \hat{a}_f^\dagger}{\sqrt{2}} \tag{I.6}$$

and give the standard commutation relations

$$\begin{aligned} [\hat{x}_f, \hat{p}_{f'}] &= \delta_{ff'} \ \imath \\ [\hat{x}_f, \hat{x}_{f'}] = [\hat{p}_f, \hat{p}_{f'}] &= 0 \end{aligned} \quad \forall \ f, f' \ . \tag{I.7}$$

2 Wigner quasiprobability distribution functions

Phase space description is often used to characterize classical physical systems, the associated distribution functions giving the probability of finding the system in a

particular state. Unfortunately this powerful approach can not be directly transcribed to quantum physical systems due to the uncertainty relations arising from the fundamental exclusivity of the observable physical quantities used in characterization of quantum physical states.

This problem may be circumvented with generalised probability distributions relaxing some of the usual requirements such as regularity and positivity. One of the possible generalisations is the Wigner quasiprobability distribution function [4, 5, 6, 22].

The Wigner function of a physical quantum state characterised by a hermitian density operator $\hat{\varrho}$ is given by Wigner's transformation formula

$$W_{\hat{\varrho}}\left(x,p\right)=\pi^{-1}\int\exp\left(2\imath p\zeta\right)\left\langle x-\zeta\left|\,\hat{\varrho}\,\right|x+\zeta\right\rangle\,\mathrm{d}\zeta\ . \tag{I.8}$$

The resulting quasiprobability distribution $W_{\hat{\varrho}}\left(x,p\right)$ is properly normalised

$$\iint W_{\hat{\varrho}}\left(x,p\right)\,\mathrm{d}x\,\mathrm{d}p=1\ , \tag{I.9}$$

the marginal probability distributions of the phase space quadratures read

$$\begin{aligned}\left\langle x\left|\,\hat{\varrho}\,\right|x\right\rangle&=\int W_{\hat{\varrho}}\left(x,p\right)\,\mathrm{d}p\\ \left\langle p\left|\,\hat{\varrho}\,\right|p\right\rangle&=\int W_{\hat{\varrho}}\left(x,p\right)\,\mathrm{d}p\ .\end{aligned} \tag{I.10}$$

The distribution associated with a physical state is regular and bounded

$$\left|W_{\hat{\varrho}}\left(x,p\right)\right|\leq\pi^{-1}\quad\forall\left(x,p\right)\in\mathbb{R}^{2}\ . \tag{I.11}$$

The Wigner function is real due to the hermicity of the density operator $\hat{\varrho}$. An overlap between two operators $\hat{\varrho}$ and $\hat{\Pi}$ is obtained using the overlap formula

$$\mathrm{Tr}\left[\hat{\varrho}\hat{\Pi}\right]=2\pi\iint W_{\hat{\varrho}}(\xi)W_{\hat{\Pi}}(\xi)\,\mathrm{d}^{2}\xi\ , \tag{I.12}$$

where the operators are not necessarily physical, i.e., normalised or regular. The transformation formula (I.8) may be extended to arbitrary multipartite operators.

Consider now a χ-partite operator $\hat{\varrho}$. Its Wigner function is obtained in the form of

$$W_{\hat{\varrho}}(\xi) = \pi^{-\chi} \int \exp(2\imath p \cdot \zeta) \langle x - \zeta \,|\, \hat{\varrho} \,|\, x + \zeta \rangle \, \mathrm{d}^{\chi}\zeta \;, \tag{I.13}$$

where the vector ξ of phase space coordinates reads

$$\xi = (x_1, p_1, \ldots, x_\chi, p_\chi)^{\intercal} \;. \tag{I.14}$$

The simple overlap formula (I.12) may be adapted to account for partial overlaps, i.e., partial traces over some subsystem γ

$$\mathrm{Tr}_{\gamma}\left[\hat{\varrho}\hat{\Pi}\right] = 2\pi \iint W_{\hat{\varrho}}(\xi) W_{\hat{\Pi}}(\xi) \, \mathrm{d}^2\xi_{\gamma} \;, \tag{I.15}$$

where the vector ξ_γ comprises the phase space coordinates of the subsystem γ

$$\xi_{\gamma} = (x_{\gamma}, p_{\gamma})^{\intercal} \;. \tag{I.16}$$

3 Gaussian states

The common definition of a Gaussian state uses the concept of Wigner functions. An arbitrary multipartite quantum state characterized by the density operator $\hat{\varrho}$ is a Gaussian state if and only if the corresponding Wigner function is a Gaussian distribution

$$W_{\hat{\varrho}}(\xi) = \frac{1}{(2\pi)^{\chi}\sqrt{\det\sigma}} \exp\left(-\frac{1}{2}(\xi - \mu)^{\intercal}\sigma^{-1}(\xi - \mu)\right) \;, \tag{I.17}$$

where χ gives the number of modes of the system. Every Gaussian state is completely characterized by its first two statistical moments, namely by its 2χ dimensional vector of mean values μ and its real, invertible, symmetric, and positive definite $2\chi \times 2\chi$ variance matrix [5, 6].

4 Gaussian operations

Gaussian operations map the set of Gaussian states onto itself. The effective Hamiltonians of such operations are at most quadratic in the quadrature operators and the Heisenberg equations essentially result in affine transformations of the quadrature operators preserving the canonical commutation relations (I.7).

The phase space coordinates (I.14) respective to the quadrature operators are transformed in the same way, following the relation

$$\xi \mapsto V\xi + \Delta \tag{I.18}$$

where V is a real $2\chi \times 2\chi$ symplectic matrix of the underlying linear transformation, its symplectic property thereby ensuring the transformation respects the commutation relations (I.7) [5, 6]. The 2χ dimensional vector Δ represents of the affine displacement.

The Wigner function of an arbitrary state $\hat{\varrho}$ transforms counter to the respective phase space transformation, i.e.,

$$W_{\hat{\varrho}}(\xi) \mapsto W_{\hat{\varrho}}(V^{-1}(\xi - \Delta)) \; . \tag{I.19}$$

The matrix V is invertible by the virtue of its symplecticity. In the case of a Gaussian state, only the respective displacement vector and the variance matrix

$$\mu \mapsto V\mu + \Delta \; , \quad \sigma \mapsto V\sigma V^{\intercal} \tag{I.20}$$

are transformed. This conclusion can be achieved by reorganizing the quadratic form within the exponential (I.17) in the chain of algebraic identities

$$\begin{gathered} (V^{-1}(\xi - \Delta) - \mu)^{\intercal}\sigma^{-1}(V^{-1}(\xi - \Delta) - \mu) = \\ (\xi - (V\mu + \Delta))^{\intercal}(V^{\intercal})^{-1}\sigma^{-1}V^{-1}(\xi - (V\mu + \Delta)) = \\ (\xi - (V\mu + \Delta))^{\intercal}(V\sigma V^{\intercal})^{-1}(\xi - (V\mu + \Delta)) \end{gathered} \tag{I.21}$$

with the aid of the matrix inverse product rule $(AB)^{-1} = B^{-1}A^{-1}$ and the inverse transpose rule $(A^{\intercal})^{-1} = (A^{-1})^{\intercal}$ in each step.

5 Measurement

Quantum physical measurement process is usually described using the **positive operator valued measure** formalism [5, 6]. The possible measurement outcomes f are associated with positive Hermitian operators $\hat{\Pi}_f$ satisfying the closure relation

$$\sum_f \hat{\Pi}_f = \hat{\mathbb{1}} \ . \tag{I.22}$$

A measurement with outcome $\hat{\Pi}_f$ performed on a single mode γ of a larger system characterized by the density operator $\hat{\varrho}$ projects the state of the remaining parts of the system onto the marginal density operator

$$\hat{\varrho}' = \mathrm{Tr}_\gamma \left[\hat{\Pi}_f \hat{\varrho}\right] \left(\mathrm{Tr}\left[\hat{\Pi}_f \hat{\varrho}\right]\right)^{-1} \ . \tag{I.23}$$

It is normalized with the probability of actually measuring the outcome $\hat{\Pi}_f$,

$$P_f = \mathrm{Tr}\left[\hat{\Pi}_f \hat{\varrho}\right] \ . \tag{I.24}$$

The above relations may be adopted in the Wigner representation using the general formula (I.15). Suppose the Wigner functions of the measured state $W_{\hat{\varrho}}(\xi)$ and the outcome element $W_{\hat{\Pi}_f}(\xi)$ are given by the relation (I.13). The Wigner function after the measurement process reads

$$W_{\hat{\varrho}'}(\xi') = \frac{\iint W_{\hat{\varrho}}(\xi) W_{\hat{\Pi}_f}(\xi) \ \mathrm{d}^2\xi_\gamma}{\iint \cdots \iint W_{\hat{\varrho}}(\xi) W_{\hat{\Pi}_f}(\xi) \ \mathrm{d}^{2\chi}\xi} \tag{I.25}$$

with the probability of the measurement outcome given by

$$P_f = 2\pi \iint \cdots \iint W_{\hat{\varrho}}(\xi) W_{\hat{\Pi}_f}(\xi) \ \mathrm{d}^{2\chi}\xi \ , \tag{I.26}$$

where the vectors of the respective phase space variables comprise

$$\begin{aligned} \xi &= (x_1, p_1, \ldots, x_\chi, p_\chi)^\intercal \ , \\ \xi' &= (x_1, p_1, \ldots, x_{\gamma-1}, p_{\gamma-1}, x_{\gamma+1}, p_{\gamma+1}, \ldots, x_\chi, p_\chi)^\intercal \ . \end{aligned} \tag{I.27}$$

6 Measures of quantum entanglement

In the decades following its inception [25], quantum entanglement has cemented its important position in many areas of research, including quantum information theory, quantum key distribution and quantum metrology. While the notion of quantum entanglement is one of the fundamental properties of quantum objects and one of the most essential resources in a myriad of applications, it is — unfortunately — incredibly hard to determine whether a quantum system is entangled or not. No entanglement criterion that would be both necessary and sufficient for a general quantum system is known to this very day. Similarly the quantification of entanglement proves to be equally challenging.

One of the most powerful tools presently available is the positive partial transpose criterion [6, 26, 27] which gives the necessary condition for separability of general multipartite quantum systems. Consequently the violation of the separability criterion may be used to measure the strength of the entanglement present in the system. The positive partial transpose condition was eventually derived for continuous variable systems [27, 28].

In particular the entanglement of bipartite Gaussian systems may be rather straightforwardly quantified with the aid of the continuous variable version of the separability condition [27, 28]. The entanglement measure

$$\Lambda = \max\left\{0, -\log \nu_-\right\} \ , \tag{I.28}$$

aptly christened **Gaussian logarithmic negativity** [27], is defined in terms of the scalar symplectic invariants

$$\begin{aligned} \Delta &= \det\alpha + \det\beta - 2\det\gamma \ , \\ \mu^2 &= \frac{1}{\det\sigma} \ , \\ \nu_\pm^2 &= 4\left(\Delta \pm \sqrt{\Delta^2 - \frac{4}{\mu^2}}\right) \end{aligned} \tag{I.29}$$

of the 4×4 variance matrix σ of the Gaussian state in consideration. The matrix

$$\sigma = \begin{pmatrix} \alpha & \gamma \\ \gamma^{\intercal} & \beta \end{pmatrix} \tag{I.30}$$

comprises four 2×2 blocks with the α and β corresponding to marginal variance matrices of the individual modes and the matrix γ representing their correlations. Furthermore the bipartite system is entangled for $\Lambda > 0$.

Another useful and quite straightforward entanglement measure is defined in the spirit of the original entanglement paper [25]. The **EPR correlations**

$$\Upsilon = \frac{1}{2}\left[\mathrm{var}(x_1 - x_2) + \mathrm{var}(p_1 + p_2)\right] \tag{I.31}$$

of a bipartite state are defined [27] as the variance of the analogues of the relative position and total momentum. The system in question is entangled for $\Upsilon < \frac{1}{2}$. The formula (I.31) rewritten in terms of the elements of the variance matrix (I.30) reads

$$\Upsilon = \frac{\mathrm{Tr}\sigma}{2} + \mathrm{cov}(p_1, p_2) - \mathrm{cov}(x_1, x_2)\ . \tag{I.32}$$

7 Overview of Gaussian states and operations

In this section we provide a brief overview of the common active and passive Gaussian operations and review several of the relevant Gaussian states and reproduce some of their properties.

A Beam splitter

Beam splitters are common elements of linear optics. An ideal beam splitter is characterised by a single parameter only — its transmittance rate. The transformation

is linear, characterized solely by the orthogonal matrix

$$V(\tau) = \begin{pmatrix} \sqrt{\tau} & \cdot & \sqrt{1-\tau} & \cdot \\ \cdot & \sqrt{\tau} & & \sqrt{1-\tau} \\ -\sqrt{1-\tau} & \cdot & \sqrt{\tau} & \cdot \\ \cdot & -\sqrt{1-\tau} & \cdot & \sqrt{\tau} \end{pmatrix} \tag{I.33}$$

with τ giving the intensity transmittance rate.

B Single mode squeezing

Gaussian operations include active optical elements such as the single mode squeezer with 2×2 transformation matrix

$$V(\gamma) = \begin{pmatrix} \exp\gamma & \cdot \\ \cdot & \exp -\gamma \end{pmatrix} . \tag{I.34}$$

where γ gives the amplification parameter.

C Two mode squeezing

The two mode squeezing operation, also known as optical parametric amplification, is an active transformation. As the name suggests, the operation acts on a pair of modes, the transformation represented by a 4×4 symplectic matrix

$$V(\gamma) = \begin{pmatrix} \cosh\gamma & \cdot & \sinh\gamma & \cdot \\ \cdot & \cosh\gamma & \cdot & -\sinh\gamma \\ \sinh\gamma & \cdot & \cosh\gamma & \cdot \\ \cdot & -\sinh\gamma & \cdot & \cosh\gamma \end{pmatrix} , \tag{I.35}$$

where γ gives the amplification parameter.

D Vacuum state

The state $|0\rangle$ is associated with the zero eigenvalue of the number operator [22]. It is only natural to expect the number of excitations to never reache negative values. Speaking in mathematical terms we expect the condition

$$\hat{a}\,|0\rangle = 0 \tag{I.36}$$

to hold. This relation may be exploited to obtain the wave function $f(x)$ of the vacuum state. Expressing the annihilation operator in terms of the canonical position and momentum operators

$$\hat{a} = \frac{\hat{x} + \imath\hat{p}}{\sqrt{2}} \tag{I.37}$$

and multiplying the condition (I.36) with $\langle x|$ from the left we arrive to an ordinary differential equation

$$\begin{aligned} \langle x\,|\,\hat{x} + \imath\hat{p}\,|\,0\rangle &= 0 \\ x\,\langle x\,|\,0\rangle + \frac{\partial}{\partial x}\,\langle x\,|\,0\rangle &= 0\,. \end{aligned} \tag{I.38}$$

The wave function $f = \langle x\,|\,0\rangle$ is obtained by solving the differential equation and enforcing the normalisation $\langle 0\,|\,0\rangle = 1$ in the exponential form

$$\begin{aligned} & xf(x) + f'(x) = 0 \\ & \implies f(x) = \frac{1}{\sqrt[4]{\pi}} \exp\left(-\frac{1}{2}x^2\right)\,. \end{aligned} \tag{I.39}$$

The Wigner function of the vacuum state is obtained directly using the transformation formula (I.8). Setting $\hat{\varrho} = |0\rangle\,\langle 0|$ we obtain the distribution in the form

$$W_{|0\rangle}(x,p) = \frac{1}{\pi}\exp\left(-x^2 - p^2\right)\,. \tag{I.40}$$

E Coherent state

Coherent states are defined [22] as the eigenstates of the annihilation operator

$$\hat{a}\,|\alpha\rangle = \alpha\,|\alpha\rangle\ , \tag{I.41}$$

with their respective eigenvalues equal to their amplitudes. Alternatively they may be described as displaced vacuum (ground) states

$$\hat{D}(\alpha)\,|0\rangle = \exp\left(\alpha\hat{a}^\dagger - \bar{\alpha}\hat{a}\right)|0\rangle = |\alpha\rangle \tag{I.42}$$

where the displacement α is equal to the desired amplitude of the coherent state. The wave function of a coherent state may be obtained directly from the first defining equation. Suppose the scaling of the complex amplitude

$$\alpha = \frac{x_0 + \imath p_0}{\sqrt{2}} \tag{I.43}$$

matches the scaling of the annihilation operator which may be expressed in terms of the canonical position and momentum operators

$$\hat{a} = \frac{\hat{x} + \imath\hat{p}}{\sqrt{2}}\ . \tag{I.44}$$

Multiplying the defining eigenvalue equation from left with $\langle x|$ and using the expression for the annihilation operator we obtain a differential equation

$$\begin{aligned} \langle x\,|\,\hat{a}\,|\,\alpha\rangle &= \langle x\,|\,\alpha\,|\,\alpha\rangle \\ \left\langle x\left|\,\frac{\hat{x}+\imath\hat{p}}{\sqrt{2}}\,\right|\alpha\right\rangle &= \left\langle x\left|\,\frac{x_0+\imath p_0}{\sqrt{2}}\,\right|\alpha\right\rangle \\ x\,\langle x\,|\,\alpha\rangle + \frac{\partial}{\partial x}\,\langle x\,|\,\alpha\rangle &= (x_0+\imath p_0)\,\langle x\,|\,\alpha\rangle\ . \end{aligned} \tag{I.45}$$

The wave function $f_\alpha(x) = \langle x\,|\,\alpha\rangle$ is obtained by solving the differential equation and enforcing the $\langle\alpha\,|\,\alpha\rangle = 1$ normalisation condition in the form

$$\begin{aligned} x f_\alpha(x) + f'_\alpha(x) &= (x_0+\imath p_0) f_\alpha(x) \\ f'_\alpha(x) &= (-x + x_0 + \imath p_0) f_\alpha(x) \\ \implies f_\alpha(x) &= \frac{1}{\sqrt[4]{\pi}} \exp\left(-\frac{(x-x_0)^2}{2} + \imath p_0 x\right)\ . \end{aligned} \tag{I.46}$$

The Wigner function of a coherent state is obtained directly using the transformation formula (I.8). Setting $\hat{\varrho} = |\alpha\rangle\langle\alpha|$ we obtain the distribution in the form

$$\begin{aligned} W_{|\alpha\rangle}(x,p) &= (\pi\sqrt{\pi})^{-1} \int \exp(2\imath p\zeta)\, \langle x-\zeta\,|\,\alpha\rangle\, \langle\alpha\,|\,x+\zeta\rangle\, \mathrm{d}\zeta \\ &= (\pi\sqrt{\pi})^{-1} \int \exp(2\imath p\zeta)\, f_\alpha(x-\zeta)\bar{f}_\alpha(x+\zeta)\, \mathrm{d}\zeta \\ &= (\pi\sqrt{\pi})^{-1} \exp\left(-\left[x-x_0\right]^2\right) \int \exp\Big(2\imath(p-p_0)\zeta\Big)\, \mathrm{d}\zeta \\ &= (\pi)^{-1} \exp\left(-(x-x_0)^2-(p-p_0)^2\right)\ . \end{aligned} \tag{I.47}$$

Alternatively the Wigner function may be obtained without any effort by displacing the vacuum state as the second definition (I.42) of the coherent state suggests. Taking the Wigner function of vacuum state and applying the phase space shift

$$x \mapsto x + x_0\ , \quad p \mapsto p + p_0 \tag{I.48}$$

we readily obtain the Wigner function in the form of

$$\begin{aligned} W_{|\alpha\rangle}(x,p) &= W_{|0\rangle}(x-x_0, p-p_0) \\ &= (\pi)^{-1} \exp\left(-(x-x_0)^2-(p-p_0)^2\right) \end{aligned} \tag{I.49}$$

where the $W_{|0\rangle}(x,p)$ denotes the Wigner function (I.40) of the vacuum state.

F Two-mode squeezed vacuum state

In the number basis the two mode squeezed vacuum state $|\Psi_\gamma\rangle$ reads

$$\begin{aligned} |\Psi_\gamma\rangle &= \hat{S}(\gamma)\,|0\rangle\,|0\rangle \\ &= \exp\Big(\bar{\gamma}\hat{a}_1\hat{a}_2 - \gamma\hat{a}_1^\dagger\hat{a}_2^\dagger\Big)\,|0\rangle\,|0\rangle \\ &= \sqrt{1-\lambda^2}\sum_{f=0}^{\infty}\lambda^f\,|f\rangle\,|f\rangle \end{aligned} \tag{I.50}$$

with the factor λ given as $\lambda = \tanh\gamma$ for real values of γ. The normalisation factor $\sqrt{1-\lambda^2}$ then equals $\operatorname{sech}\gamma$, rendering the formula

$$|\Psi_\gamma\rangle = \frac{1}{\cosh\gamma}\sum_{f=0}^{\infty}(\tanh\gamma)^f\,|f\rangle\,|f\rangle \ . \tag{I.51}$$

Because the two-mode squeezing operation is Gaussian, the Wigner function of the state is Gaussian and may obtained in a straightforward fashion by applying the two mode squeezing operation (I.35) on a two mode vacuum state. The variance matrix σ of the two-mode squeezed vacuum state therefore reads

$$\sigma = 2^{-1}\begin{pmatrix} \cosh 2\gamma & \cdot & \sinh 2\gamma & \cdot \\ \cdot & \cosh 2\gamma & \cdot & -\sinh 2\gamma \\ \sinh 2\gamma & \cdot & \cosh 2\gamma & \cdot \\ \cdot & -\sinh 2\gamma & \cdot & \cosh 2\gamma \end{pmatrix} \ . \tag{I.52}$$

Chapter II

Improved subtraction procedure

In our previous work [19] we focused our attention on the single photon subtraction [13, 14] and proposed an improved version of the subtraction procedure with the intention of enhancing its success rate along with improving its general performance. In this chapter we briefly review both the original and the improved subtraction procedures and develop a general description in the Wigner representation.

1 Original subtraction procedure

In its original conception (depicted in the Figure II.1a) the subtraction procedure transformed the signal mode by tapping off a fragment of light using a strongly unbalanced beam splitter. The reflected fragment was then measured using an ideal on-off detector and the procedure was considered successful if and only if the detector clicked, i.e., the fragment of light was registered by the detector.

In order to model detectors of limited quantum efficiency a slight modification to the scheme (*cf.* Figure II.1b) was made, namely a virtual beam splitter and a virtual ancillary mode were added to account for the losses due to the inefficiencies. The detailed description of the revised procedure may be formally divided into the following four logical units.

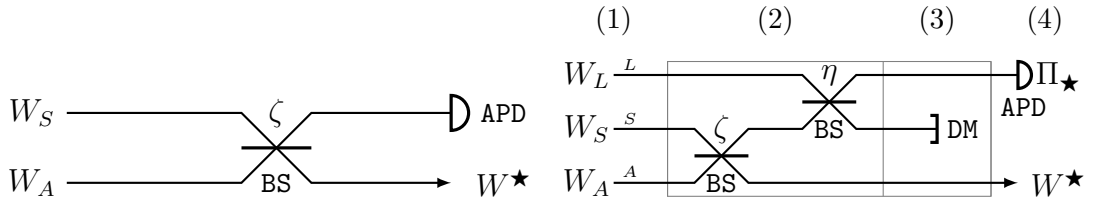

(a) Ideal detection **(b)** Realistic, inefficient detection

Figure II.1: The signal mode (S) interacts with an empty idler (A) on the primary beam splitter of high transmittance ζ. A fragment of light is reflected into the idler, which is then measured using an on-off detector. The subtraction is considered successful if the detector clicks. The output Wigner function $W^\star$ represents both possible outcomes.

The on-off detector used in the part **(a)** is an ideal avalanche photodiode (APD). The inefficient APD in the part **(b)** is modelled using a virtual beam splitter and a virtual ancillary mode (L). The virtual mode interacts with the idler (A) on the virtual beam splitter with transmittance η equal to the quantum efficiency of the APD. The virtual mode is discarded right away, representing the losses due to the reduced efficiency.

(1) The input signal mode is prepared in an arbitrary state (W_S), while both the idler and the virtual mode are prepared in vacuum states (W_A, W_L). The Wigner function of the joint state is factorized, obtained as a product of their respective Wigner functions

$$W_{SAL}(\xi) = W_S(\xi_S) W_A(\xi_A) W_L(\xi_L) \,, \tag{II.1}$$

with the vector of phase space coordinates given by the direct sum

$$\begin{aligned} \xi &= \xi_S \oplus \xi_A \oplus \xi_L \\ &= (x_S, p_S, x_A, p_A, x_L, p_L)^\intercal \end{aligned} \tag{II.2}$$

of the individual phase space coordinate pairs $\xi_S = (x_S, p_S)^\intercal$, $\xi_A = (x_A, p_A)^\intercal$ and $\xi_L = (x_L, p_L)^\intercal$.

(2) The signal mode interacts with the idler mode on the (primary) beam splitter of transmittance $\zeta \in (0, 1)$. The transmittance ratio affects the amount of light reflected into the idler, which in turn affects the quality of the approximation of the annihilation operator and consequently the probability of successful

subtraction. Similarly the idler then interacts with the virtual mode on the virtual beam splitter of transmittance $\eta \in (0, 1)$, the virtual transmittance ratio equal to the quantum efficiency of the realistic detector.

Both the interactions are Gaussian operations, each resulting in a linear transformation (I.33) of the quadrature coordinates. Because a sequence of Gaussian operations is a Gaussian operation itself, the effect of the interactions may be described with a single transformation matrix

$$V(\zeta, \eta) = [\mathbb{1} \oplus V(\eta)]\,[V(\zeta) \oplus \mathbb{1}] \tag{II.3}$$

obtained as a properly padded product of the individual transformation matrices, where $\mathbb{1}$ denotes a 2×2 identity matrix. The joint Wigner function transforms accordingly into

$$W'_{SAL}(\xi) = W_{SAL}(V(\zeta, \eta)^{-1}\xi) \tag{II.4}$$

following the relation (I.19) governing Gaussian operations.

(3) The virtual idler is discarded, representing the losses due to the detector inefficiency. This is equal to tracing the respective mode out, i.e., projecting it onto the respective identity operator $\hat{\mathbb{1}}$. With the aid of the formula (I.15) for partial traces we readily obtain the marginal Wigner function

$$W'_{SA} = \iint W'_{SAL}(\xi)\ \mathrm{d}^2\xi_L \tag{II.5}$$

where the vector of phase space coordinates ξ reduces into

$$\begin{aligned} \xi &= \xi_S \oplus \xi_A \\ &= (x_S, p_S, x_A, p_A)^{\intercal}\ . \end{aligned} \tag{II.6}$$

It is worth remarking that the probability associated with the $\hat{\mathbb{1}}$ projection takes the intuitively expected value

$$P = \iint \iint \iint W'_{SAL}(\xi)\ \mathrm{d}^2\xi_S\ \mathrm{d}^2\xi_A\ \mathrm{d}^2\xi_L = 1 \tag{II.7}$$

since $W'_{SAL}(\xi)$ describes a normalised physical state of the post-interaction

system.

(4) The measurement of the idler determines whether the subtraction procedure was successful. An ideal avalanche photodiode is utilized in the detection process, its inefficiencies already contained within the W'_{SA} state. The measurement process is completely characterized with a pair of positive operator measure elements. The negative outcome is associated with the projection on the vacuum state, represented by the operator

$$\hat{\Pi}_{\circ} = |0\rangle \langle 0| \ , \tag{II.8}$$

while the positive outcome (click) is associated with the operator

$$\begin{aligned} \hat{\Pi}_{\bullet} &= \hat{\mathbb{1}} - |0\rangle \langle 0| \\ &= \hat{\mathbb{1}} - \hat{\Pi}_{\circ} \ . \end{aligned} \tag{II.9}$$

The Wigner function respective to the negative outcome element reads

$$\begin{aligned} W_{\hat{\Pi}_{\circ}}(\xi_A) &= \pi^{-1} \exp\left(-x_A^2 - p_A^2\right) \\ &= \pi^{-1} \exp\left(-\xi_A^{\intercal} \xi_A\right) \ . \end{aligned} \tag{II.10}$$

The Wigner function $W_{\hat{\Pi}_{\circ}}(\xi_A)$ is clearly Gaussian and properly normalised. Similarly the Wigner function respective to the positive outcome reads

$$\begin{aligned} W_{\hat{\Pi}_{\bullet}}(\xi_A) &= (2\pi)^{-1} - \pi^{-1} \exp\left(-x_A^2 - p_A^2\right) \\ &= (2\pi)^{-1} - \pi^{-1} \exp\left(-\xi_A^{\intercal} \xi_A\right) \ . \end{aligned} \tag{II.11}$$

This Wigner function is not normalised as it no longer represents a physical state. The subtraction procedure is considered **successful** if the positive detection outcome occurs. The probability of this detection event reads

$$P^{\bullet} = 2\pi \iint \iint W'_{SA}(\xi) W_{\hat{\Pi}_{\bullet}}(\xi_A) \ \mathrm{d}^2\xi_A \ \mathrm{d}^2\xi_S \ . \tag{II.12}$$

Consequently the Wigner function of the successfully subtracted state takes the standard form (I.25), resulting in

$$W^{\bullet}(\xi_S) = \frac{\iint W'_{SA}(\xi) W_{\hat{\Pi}_{\bullet}}(\xi_A) \ \mathrm{d}^2\xi_A}{\iint \iint W'_{SA}(\xi) W_{\hat{\Pi}_{\bullet}}(\xi_A) \ \mathrm{d}^2\xi_A \ \mathrm{d}^2\xi_S} \ . \tag{II.13}$$

The converse detection outcome advertises the subtraction procedure was indeed **unsuccessful**. The probability is given as

$$P^{\circ} = 2\pi \iint \iint W'_{SA}(\xi) W_{\hat{\Pi}_{\circ}}(\xi_A) \, \mathrm{d}^2\xi_A \, \mathrm{d}^2\xi_S \, , \tag{II.14}$$

while the Wigner function of the unsuccessfully subtracted state reads

$$W^{\circ}(\xi_S) = \frac{\iint W'_{SA}(\xi) W_{\hat{\Pi}_{\circ}}(\xi_A) \, \mathrm{d}^2\xi_A}{\iint \iint W'_{SA}(\xi) W_{\hat{\Pi}_{\circ}}(\xi_A) \, \mathrm{d}^2\xi_A \, \mathrm{d}^2\xi_S} \, . \tag{II.15}$$

2 Improved subtraction procedure

In our previous work an improved version of the original subtraction procedure was proposed with the intention of enhancing its success rate [19].

The central idea of the improved method lies in the way the unsuccessful subtraction attempts are handled. In contrast with the original protocol, where the output is simply discarded if the subtraction fails, we keep recycling the unsuccessfully subtracted states until the procedure either succeeds or a reasonable, predetermined number of attempts is eventually reached.

The basic outline of the improved subtraction procedure is presented in the Figure II.2. In the depicted iterative chain the first $1 \ldots (f-1)$ subtraction attempts fail before ultimately succeeding in the final iteration f. The conditional probability

$$\begin{aligned} P_f &= P_1^{\circ} \cdots P_{f-1}^{\circ} P_f^{\bullet} \\ &= P_1^{\circ} \cdots P_{f-1}^{\circ} (1 - P_f^{\circ}) \end{aligned} \tag{II.16}$$

associated with the iterative chain represents the first $(f-1)$ failures followed by the final success, the individual probabilities P° and $P^{\bullet}$ given by (II.14) and (II.12).

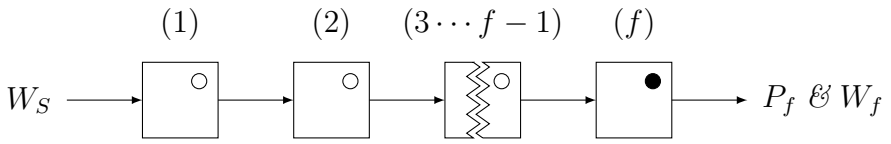

Figure II.2: When the subtraction procedure fails, the output is iteratively recycled until the procedure finally succeeds.

In the presented case, the procedure succeeds in the fth attempt. The conditional probability associated with this iterative chain is denoted P_f, the respective Wigner function of the output state W_f.

The number of subtraction attempts is not indefinite. The maximal number of iteration steps, albeit arbitrary, reflects the properties of the signal state, the characteristics of the subtraction procedure (detection efficiency, primary beam splitter transmittance) and other constraints such as timing requirements.

The improved subtraction procedure either succeeds in any of the iterations under consideration or it fails completely. Because the first successful iteration is not known beforehand, we take all the possible iterative chains into account.

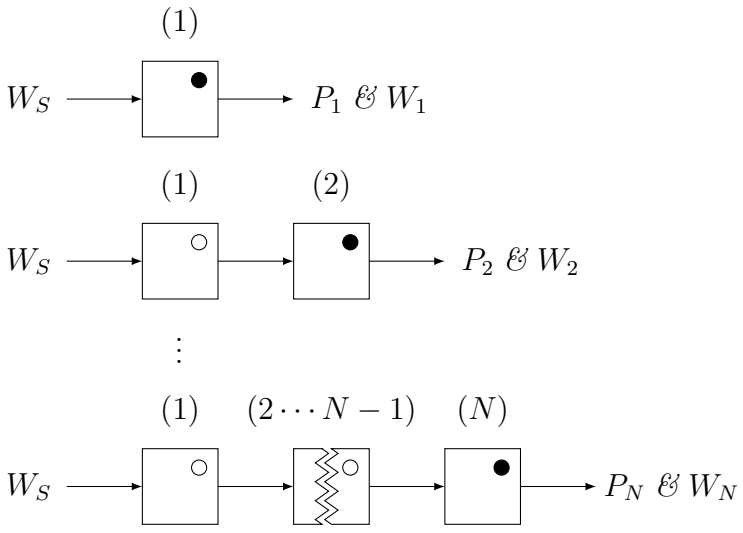

Figure II.3: Each line shows a single iterative chain where the subtraction succeeds in different iteration. On the first line the subtraction succeeds in the 1st attempt, on the second line in the 2nd one. A number of iterative steps in the range of $3 \ldots (N-1)$ is omitted. Finally the iterative chain depicted on the last line succeeds in the Nth attempt.

This approach is outlined in the Figure II.3 where each line represents an iterative chain where the subtraction succeeds in different iteration. Each of the iterative chains is statistically independent. The overall probability of the improved subtraction procedure succeeding is therefore obtained in the additive form

$$Q_N = \sum_f^N P_f \ , \tag{II.17}$$

where N represents the maximal number of subtraction attempts. The individual probabilities P_f of the iterative chains are given by the formula (II.16). The overall Wigner function emerges as a weighted average

$$W_N(\xi_S) = Q_N^{-1} \sum_f^N P_f W_f(\xi_S) \tag{II.18}$$

over the entire statistical ensemble. In essence we have traded the eventual state purity for the increased probability of success of the subtraction procedure.

Chapter III

Improved mathematical formulation

The previous chapter concentrated on a brief review of the original subtraction protocol and on a proposal of an improvement aiming to increase the subtraction probability at the expense of purity of the output state. The central idea of the improvement was an iterative application of the original subtraction procedure and an evaluation of the resulting statistical ensemble.

We derived a number of relations (II.12), (II.13), (II.14), (II.15), (II.17), and (II.18) describing both the original and the improved subtraction procedures in a general Wigner representation.

Our further analysis of the improved procedure relies heavily on Gaussian states, rendering the use of fully general Wigner functions an unnecessary complication. This is thoroughly addressed in this chapter, where we introduce a simpler description based on Wigner functions of Gaussian states and their linear combinations. We also aim to provide an approach guaranteeing a fast, numerically stable solutions in the numerical simulations used in chapters IV and V.

The mathematical framework is built incrementally in the following sections to suit both the original and the improved subtraction procedures. We start with a description (section III.1) based solely on Gaussian Wigner functions and quickly discover it is incomplete as it fails to cover the successfully subtracted states. We overcome this issue by taking an alternative approach (section III.2) and show the class of

states under our consideration forms a complete set in respect to both the original and the improved subtraction procedures.

1 Keeping up with the Gaussians

In the spirit of the original procedure we start our investigation with Gaussian signal states. We start with a single mode squeezed vacuum state and examine each part of the original subtraction procedure depicted in the Figure II.1b.

(1) The first part of the procedure consists of preparation only. The product state is Gaussian, the joint variance matrix

$$\sigma = \sigma_S \oplus \sigma_A \oplus \sigma_L \tag{III.1}$$

is obtained in the form of a block-diagonal matrix as the modes do not interact with each other at this time.

(2) In the second part the modes of the system interact with each other. The interaction is Gaussian, resulting in a transformation of the phase space coordinates (I.18). The interaction is completely characterized by the orthogonal matrix (II.3). The joint Gaussian state is transformed accordingly, its variance matrix mapped into

$$\sigma_{SAL} \mapsto V(\zeta, \eta)\sigma_{SAL}V(\zeta, \eta)^{\intercal} \tag{III.2}$$

as the relation (I.20) suggests.

(3) Nothing notable happens in the third part. The projection onto the identity operator preserves the Gaussian nature of the state. The rows and columns of the variance matrix (and the rows of the vector of mean values) pertaining to the virtual mode are simply removed, yielding the marginal variance σ_{SA}.

(4) The negative outcome element (II.10) is clearly Gaussian as the projection operator is identical to the density operator of vacuum state. The product of the two Gaussian Wigner functions in the relation (II.15) reads

$$\exp\left(-\frac{1}{2}\xi_{SA}^{\intercal}\sigma_{SA}^{-1}\xi_{SA}\right)\exp\left(-\frac{1}{2}\xi_{A}^{\intercal}\gamma_{A}^{-1}\xi_{A}\right) \tag{III.3}$$

with the variance matrix of the vacuum projector $\hat{\Pi}_\circ$ denoted γ_A. The inverse matrix γ_A^{-1} must be zero-padded to match the dimension of the σ_{SA}^{-1} matrix in order for them to be added together, giving an augmented variance matrix of the product Gaussian state

$$\sigma = \left(\sigma_{SA}^{-1} + \left[\mathrm{diag}(0,0) \oplus \gamma_A^{-1}\right]\right)^{-1} \ . \tag{III.4}$$

The overlap integral preserves the Gaussian nature of the output state, the variance matrix σ is stripped of the rows and columns related to the ancillary mode, yielding the resulting variance matrix σ°.

The positive outcome element (II.11) is not Gaussian as it consists of two operators. The first one, an identity operator, results in a behaviour formally identical to the part (3) of this analysis. The other operator is equal to the previously described negative outcome projector (II.10). The Wigner function (II.13) of the output state is therefore a properly normalised weighted linear combination of two Gaussian functions with variance matrices σ_{SA} and σ°.

In conclusion a Gaussian signal state remains Gaussian if the subtraction procedure fails. Conversely it becomes a linear combination of Gaussian functions if the subtraction procedure succeeds.

2 Journey beyond Gaussian states

The improved subtraction procedure serves as a key element of the entanglement distillation protocol described in chapter V. The protocol works with a two mode squeezed vacuum state. In essence the subtraction procedure is repeatedly applied on one of the entangled arms until it either succeeds or some arbitrary number of attempts is reached. Once successful, the same process is repeated for the other arm.

This mode of operation inevitably leads to a fundamental issue after the first successful subtraction as the state is no longer Gaussian, yet the subtraction has to be repeated for the other arm. The current description of the procedure is therefore insufficient and has to be extended to support more general signal states.

We have to, at least, consider signal states that may be expressed as weighted linear

combinations of Gaussian functions

$$W_S(\xi_S) = \sum_f \gamma_f G_{\sigma_f}(\xi_S) \tag{III.5}$$

with the weights $\gamma_f \in \mathbb{R}$ adding up to unity to preserve the normalisation of the Wigner function. The individual Gaussian function $G_\sigma(\xi)$ is defined as

$$G_\sigma(\xi) = \frac{1}{(2\pi)^\chi \sqrt{\det \sigma}} \exp\left(-\frac{1}{2}\xi^\intercal \sigma^{-1} \xi\right) , \tag{III.6}$$

where χ represents the number of modes in the signal state.

Unfortunately this decomposition is not suitable for the Wigner functions (II.10) and (II.11) of the negative and positive detection outcomes. Furthermore this decomposition requires a large amount of inversion operations, making it unsuitable due to reduced numerical stability and increased computational complexity.

A Gaussian kernel decomposition

While the approach outlined in (III.5) is a good idea in general, it can not describe the Wigner functions of the detection outcomes. A slightly broader class of Wigner functions is therefore required.

Consider a generalisation of the Gaussian decomposition (III.5) where the Wigner function decomposes into a linear combination

$$W(\xi) = \sum_f \gamma_f K_{\Theta_f}(\xi) \tag{III.7}$$

of weighted **Gaussian kernels** $K_\Theta(\xi)$ defined by the relation

$$K_\Theta(\xi) = \exp\left(-\frac{1}{2}\xi^\intercal \Theta \xi\right) , \tag{III.8}$$

where the **characteristic matrix** Θ is symmetrical and not necessarily regular. The matrix characterizes each Gaussian kernel completely. Gaussian functions and

Gaussian kernels are closely related. In fact the following identity

$$G_\sigma(\xi) = \frac{1}{(2\pi)^\chi \sqrt{\det \sigma}} K_{\sigma^{-1}}(\xi) \quad \forall G_\sigma(\xi) \tag{III.9}$$

holds for every Gaussian function as the inverse of the variance matrix exists. The converse relation **does not hold in general**, i.e., not every Gaussian kernel has a Gaussian function counterpart.

This is actually quite beneficial to our use case because it allows us to express certain singular Wigner functions in terms of Gaussian kernels. Consider the Wigner function of the identity operator

$$\begin{aligned} W_{\hat{\mathbb{1}}}(x,p) &= \pi^{-1} \int \exp(2\imath p\zeta) \, \langle x - p \,|\, x + p \rangle \, \mathrm{d}\zeta \\ &= \pi^{-1} \int \exp(2\imath p\zeta) \, \delta(2\zeta) \, \mathrm{d}\zeta \\ &= (2\pi)^{-1} \end{aligned} \tag{III.10}$$

obtained using the general definition (I.8). Clearly this Wigner function does not represent a physical state. It is not Gaussian, however, it may be easily represented using the decomposition formula (III.7) with a single kernel, its respective weight and the singular characteristic matrix reading

$$\gamma = (2\pi)^{-1} \,, \quad \Theta = \mathrm{diag}(0,0) \,. \tag{III.11}$$

We may also easily express both the relations (II.10) and (II.11) in these terms. The weight and the regular characteristic matrix of (II.10) are easily obtained as

$$\gamma^\circ = \pi^{-1} \,, \quad \Theta^\circ = \mathrm{diag}(2,2) \,, \tag{III.12}$$

while the weights and characteristic matrices of the positive outcome (II.11) read

$$\begin{aligned} \gamma_1^\bullet &= (2\pi)^{-1} \,, & \Theta_1^\bullet &= \mathrm{diag}(0,0) \,, \\ \gamma_2^\bullet &= -\pi^{-1} \,, & \Theta_2^\bullet &= \mathrm{diag}(2,2) \,. \end{aligned} \tag{III.13}$$

B Original subtraction procedure revisited

Equipped with these observations we follow the white rabbit down the hole. Once again we are going to follow the path we took in the previous section and examine the effects each part of the subtraction procedure has on the class of states in our consideration. We are going to develop the necessary mathematical formulae on our journey through the original subtraction procedure depicted in the Figure II.1b.

(1) The states are prepared in the first part of the procedure. The joint state

$$W_{SAL}(\xi) = W_S(\xi_S)W_A(\xi_A)W_L(\xi_L) \tag{III.14}$$

is obtained as a product of the individual Wigner functions characterising the signal, the idler and the virtual ancillary modes. Assuming that the signal mode is characterized by the relation (III.7), the joint Wigner function reads

$$W_{SAL}(\xi) = \sum_f \gamma_f K_{\Theta_f}(\xi) \tag{III.15}$$

with the weights γ_f obtained as a product of the individual weights

$$\begin{aligned} \gamma_f &= \gamma_f^S \gamma^A \gamma^L \\ &= \gamma_f^S \pi^{-2} \ . \end{aligned} \tag{III.16}$$

The joint characteristic matrix written in the form of direct matrix sum

$$\Theta_f = \Theta_f^S \oplus \Theta^A \oplus \Theta^L \ = \Theta_f^S \oplus \mathrm{diag}(2,2) \oplus \mathrm{diag}(2,2) \ . \tag{III.17}$$

(2) In the second part the modes of the system interact with each other. The interaction is Gaussian, the transformation completely characterized by the orthogonal matrix (II.3).

The joint Wigner function transforms according to the formula (I.19) into

$$W_{SAL}(V(\zeta,\eta)^{-1}\xi) = \sum_f \gamma_f K_{\Theta_f}(V(\zeta,\eta)^{-1}\xi) \ , \tag{III.18}$$

where the effect of the phase space transformation propagates down to the in-

dividual Gaussian kernels. The exponential argument of an arbitrary Gaussian kernel $K_\Theta(\xi)$ defined in (III.8) transforms into

$$\begin{aligned}(V^{-1}\xi)^\intercal\Theta(V^{-1}) &= \xi^\intercal(V^{-1})^\intercal\Theta V^{-1}\xi \\ &= \xi^\intercal V\Theta V^\intercal\xi\end{aligned} \tag{III.19}$$

assuming the transformation matrix V is **orthogonal**. This shows that the characteristic matrix Θ transforms in the same way a variance matrix would,

$$\Theta \mapsto V\Theta V^\intercal \ . \tag{III.20}$$

The joint Wigner function (III.18) therefore undergoes the transformation on the level of individual characteristic matrices of the Gaussian kernels

$$\begin{aligned}W'_{SAL}(\xi) &= \sum_f \gamma_f K_{V(\zeta,\eta)\Theta_f V(\zeta,\eta)^\intercal}(\xi) \\ &= \sum_f \gamma_f K_{\Theta'_f}(\xi) \ ,\end{aligned} \tag{III.21}$$

where each characteristic matrix transforms according to (III.20) into

$$\Theta'_f = V(\zeta,\eta)\Theta_f V(\zeta,\eta)^\intercal \ . \tag{III.22}$$

However, the transformation matrix V characterizing the Gaussian operation is not orthogonal in general, it is merely symplectic. In the general case the transformation of the characteristic matrix is governed by the relation

$$\Theta \mapsto (V^{-1})^\intercal\Theta V^{-1} \ , \tag{III.23}$$

where the inverse of the transformation matrix V is no longer necessarily equal to its transposition. In the following, the simple relation (III.20) holds as only the beam splitter interactions (I.33) are involved. For instance neither transformation matrix of the active Gaussian operations (I.34) nor (I.35) is orthogonal as both involve scaling of the phase space.

(3) The state (III.21) is essentially projected onto the identity operator associated with the virtual ancillary mode.

In a general case we would be looking at the product of two Wigner functions

$$\begin{aligned} W_{\hat{\varrho}}(\xi)W_{\hat{\Pi}}(\xi) &= \sum_f \sum_{f'} \gamma_f \vartheta_{f'} K_{\Theta_f}(\xi) K_{\Omega_{f'}}(\xi) \\ &= \sum_f \sum_{f'} \gamma_f \vartheta_{f'} K_{\Xi_{ff'}}(\xi) \ , \end{aligned} \tag{III.24}$$

where the product of two Gaussian kernels $K_{\Theta_f}(\xi)$ and $K_{\Omega_{f'}}(\xi)$ reads

$$\begin{aligned} K_{\Theta_f}(\xi)K_{\Omega_{f'}}(\xi) &= \exp\left(-\xi^{\mathsf{T}}\Theta_f\xi\right)\exp\left(-\xi^{\mathsf{T}}\Omega_{f'}\xi\right) \\ &= \exp\left(-\xi^{\mathsf{T}}(\Theta_f + \Omega_{f'})\xi\right) \\ &= \exp\left(-\xi^{\mathsf{T}}\Xi_{ff'}\xi\right) \\ &= K_{\Xi_{ff'}}(\xi) \ . \end{aligned} \tag{III.25}$$

Here the Wigner function (III.11) of the identity operator consists of a single, constant element $\gamma = (2\pi)^{-1}$ only. The partial trace integral (I.15) therefore boils down to the expression

$$W_{SA}(\xi) = \iint W'_{SAL}(\xi)\ \mathrm{d}^2\xi_L = \sum_f \gamma_f \iint K_{\Theta'_f}(\xi)\ \mathrm{d}^2\xi_L \ , \tag{III.26}$$

that is into a sum of planar integrals of the individual Gaussian kernels $K_{\Theta'_f}(\xi)$ over the virtual ancillary mode ($\mathrm{d}^2\xi_L$).

We are going to derive the formulae describing integral transformations such as the one recently introduced in (III.26). We start our derivation with a single dimensional integral over an arbitrary one dimensional subspace of the phase space and then move to planar, two dimensional subspaces. Consider a particular Gaussian kernel $K_\Theta(\xi)$ and suppose the integration is performed over the fth phase space variable, that is over the ξ_f

$$\int K_\Theta(\xi)\ \mathrm{d}\xi_f = \int \exp\left(-\frac{1}{2}\xi^{\mathsf{T}}\Theta\xi\right)\ \mathrm{d}\xi_f \ . \tag{III.27}$$

The integration preserves the exponential nature of the kernel, the integral

transformation reading

$$\int \exp\left(-\frac{1}{2}\xi^{\intercal}\Theta\xi\right)\,\mathrm{d}\xi_f \mapsto \sqrt{\frac{2\pi}{\Theta_{ff}}}\exp\left(-\frac{1}{2}\xi^{\intercal}\Theta'\xi\right)\ , \tag{III.28}$$

where the integration induces a non-linear transformation $\Theta \mapsto \Theta'$ of the characteristic matrix

$$\Theta'_{ij} = \Theta_{ij} - \frac{\Theta_{if}\Theta_{fj}}{\Theta_{ff}} \quad \forall\,(i,j)\ . \tag{III.29}$$

It also produces a multiplicative factor proportional to the diagonal element Θ_{ff} respective to the integration variable. These results follow from the chain

$$\begin{aligned}
\int \exp\left(-\frac{1}{2}\xi^{\intercal}\Theta\xi\right)\,\mathrm{d}\xi_f &= \\
\int \exp\left(-\frac{1}{2}\sum_i\sum_j \xi_i\Theta_{ij}\xi_j\right)\,\mathrm{d}\xi_f &= \\
\int \exp\left(-\frac{1}{2}\Theta_{ff}\xi_f^2 - \xi_f\sum_{i\neq f}\xi_i\Theta_{if} - \frac{1}{2}\sum_{i\neq f}\sum_{j\neq f}\xi_i\Theta_{ij}\xi_j\right)\,\mathrm{d}\xi_f &= \\
\exp\left(-\frac{1}{2}\sum_{i\neq f}\sum_{j\neq f}\xi_i\Theta_{ij}\xi_j\right)\int \exp\left(-\frac{1}{2}\Theta_{ff}\xi_f^2 - \xi_f\sum_{i\neq f}\xi_i\Theta_{if}\right)\,\mathrm{d}\xi_f &= \\
\sqrt{\frac{2\pi}{\Theta_{ff}}}\exp\left(-\frac{1}{2}\sum_{i\neq f}\sum_{j\neq f}\xi_i\Theta_{ij}\xi_j + \frac{1}{2}\left[\sum_{i\neq f}\xi_i\Theta_{if}\right]^2\right) &= \\
\sqrt{\frac{2\pi}{\Theta_{ff}}}\exp\left(-\frac{1}{2}\sum_{i\neq f}\sum_{j\neq f}\xi_i\left[\Theta_{ij} - \frac{\Theta_{if}\Theta_{fj}}{\Theta_{ff}}\right]\xi_j\right)&
\end{aligned} \tag{III.30}$$

of identities employing the Gaussian integral formulae and the symmetry of the characteristic matrix Θ.

Strictly speaking the integral map (III.28) is valid only in combination with the relation (III.29) as the integration variable ξ_f remains on the right side of the integral mapping. This could pose a formal issue, however, the elements

of the characteristic matrix pertaining to the integration variables cancel out by the virtue of the relation (III.29)

$$\Theta'_{if} = \Theta_{if} - \frac{\Theta_{if}\Theta_{ff}}{\Theta_{ff}} = \Theta_{if} - \Theta_{if} = 0 \quad \forall i \tag{III.31}$$

effectively removing the integration variable ξ_f from the right hand side.

The planar integral is acquired with some effort using the relation (III.29) twice. Assuming the integration is performed over the variables ξ_f and $\xi_{f'}$, the integral transformation formula reads

$$\iint \exp\left(-\frac{1}{2}\xi^{\intercal}\Theta\xi\right) \mathrm{d}\xi_f \, \mathrm{d}\xi_{f'} \mapsto \frac{2\pi}{\sqrt{\Theta'_{f'f'}\Theta_{ff}}} \exp\left(-\frac{1}{2}\xi^{\intercal}\Theta''\xi\right) , \tag{III.32}$$

which may be further improved. After a little algebraic endeavour we obtain the numerator of the multiplicative factor in the relation (III.32) as

$$\Theta_{ff}\Theta'_{f'f'} = \Theta_{ff}\Theta_{f'f'} - \Theta_{ff'}\Theta_{f'f} \tag{III.33}$$

and a slightly more convoluted formulation of the matrix transformation

$$\begin{aligned}\Theta''_{ij} = \Theta_{ij} - \frac{\Theta_{if}\Theta_{fj}}{\Theta_{ff}} - \frac{\Theta_{ff}}{\Theta_{ff}\Theta_{f'f'} - \Theta_{ff'}\Theta_{gf}} \times \\ \left(\Theta_{if'} - \frac{\Theta_{if}\Theta_{ff'}}{\Theta_{ff}}\right)\left(\Theta_{f'j} - \frac{\Theta_{f'f}\Theta_{fj}}{\Theta_{ff}}\right)\end{aligned} \quad \forall\,(i,j)\ . \tag{III.34}$$

With some additional effort we may come to the conclusion we are already familiar with: the rows and columns corresponding to ξ_f and $\xi_{f'}$ cancel out.

The planar integrals we are interested in are performed over phase space variables related to specific modes of the system. For instance the planar integral in (III.26) relates to the virtual ancillary mode, i.e., to the vector $\xi_L = (x_L, p_L)^{\intercal}$ of phase space variables.

In conclusion, the planar integral transformation of a general Gaussian kernel

$K_\Theta(\xi)$ over the χth mode of the system simply reads

$$\iint \exp\left(-\frac{1}{2}\xi^\intercal\Theta\xi\right)\,\mathrm{d}^2\xi_\chi \mapsto \frac{2\pi}{\sqrt{\det\lfloor\Theta\rceil_\chi}}\exp\left(-\frac{1}{2}\xi^\intercal\Theta''\xi\right)\,, \tag{III.35}$$

with Θ'' defined by the relation (III.34), where the symbol $\lfloor\Theta\rceil_\chi$ denotes the 2×2 submatrix respective to the χth mode.

The formula (III.35) applied onto the expression (III.26) therefore yields

$$W_{SA}(\xi) = \sum_f \gamma_f \frac{2\pi}{\det\lfloor\Theta'_f\rceil_L} K_{\Theta''_f}(\xi) = \sum_f \gamma''_f K_{\Theta''_f}(\xi) \tag{III.36}$$

with the Θ''_f obtained using (III.34) and the associated γ''_f factors reading

$$\gamma''_f = \gamma_f \frac{2\pi}{\det\lfloor\Theta'_f\rceil_L}\,. \tag{III.37}$$

(4) The idler is measured in the final part of the subtraction procedure. Fortunately we have already collected all the necessary formulae. We use the product formula (III.24) and the overlap relation (III.35) to our advantage for both the positive and the negative outcomes in the detection processes.

We have already performed a rather similar derivation in the previous stage with the virtual ancillary mode where we have projected onto the identity operator (III.11).

In essence the measurement process results in a projection of the state either onto the positive (III.13) or the negative (III.12) outcome elements in the measured mode. Consequently the weights in the resulting linear combination change and the output state must be renormalised as the original transformation relations (II.13) and (II.15) suggest.

In our further treatment of the detection process we introduce an abstract version of the relations (II.13), (II.12), (II.15), and (II.14) governing the probability and the resulting Wigner function respective to the positive and negative

outcomes

$$W^{\bigstar}(\xi_S) = \frac{\iint W'_{SA}(\xi) W_{\hat{\Pi}_{\bigstar}}(\xi)\ \mathrm{d}^2\xi_A}{\iint\iint W'_{SA}(\xi) W_{\hat{\Pi}_{\bigstar}}(\xi)\ \mathrm{d}^2\xi_A\ \mathrm{d}^2\xi_S}\ ,$$
$$P^{\bigstar} = (2\pi) \iint\iint W'_{SA}(\xi) W_{\hat{\Pi}_{\bigstar}}(\xi)\ \mathrm{d}^2\xi_A\ \mathrm{d}^2\xi_S \tag{III.38}$$

where the symbols $\bigstar \in \{\bullet, \circ\}$ represent both the negative and positive detection outcomes. In the following paragraphs we presume the Wigner functions of the detection outcomes decompose into

$$W_{\hat{\Pi}_{\bigstar}}(\xi) = \sum_{f'} \gamma^{\bigstar}_{f'} K_{\Theta^{\bigstar}_{f'}}(\xi) \tag{III.39}$$

with the concrete characteristic matrices $\Theta^{\bigstar}_{f'}$ and weights $\gamma^{\bigstar}_{f'}$ given by the relations (III.12) and (III.13).

Starting with the probability formula $P^{\bigstar}$ and following the intermediate Wigner function (III.36) from the previous step we observe

$$\begin{aligned} P^{\bigstar} &= 2\pi \iint\iint \sum_{f} \sum_{f'} \gamma''_f \gamma^{\bigstar}_{f'} K_{\Theta''_f}(\xi) K_{\Theta^{\bigstar}_{f'}}(\xi)\ \mathrm{d}^2\xi_A\ \mathrm{d}^2\xi_S \\ &= 2\pi \sum_{f} \sum_{f'} \gamma''_f \gamma^{\bigstar}_{f'} \iint K_{\Xi_{ff'}}(\xi)\ \mathrm{d}^2\xi_A\ \mathrm{d}^2\xi_S \\ &= (2\pi)^3 \sum_{f} \sum_{f'} \frac{\gamma''_f \gamma^{\bigstar}_{f'}}{\sqrt{\det \Xi_{ff'}}} \end{aligned} \tag{III.40}$$

with the aid of the relation (III.24) giving the joint characteristic matrices

$$\Xi_{ff'} = \Theta''_f + \Theta^{\bigstar}_{f'} \tag{III.41}$$

and the integral formula (III.35) used in the last step. The Wigner function

$W^\star(\xi)$ is obtained in a similar fashion

$$W^\star(\xi_S) = \frac{\iint \sum_f \sum_{f'} \gamma''_f \gamma^\star_{f'} K_{\Theta''_f}(\xi) K_{\Theta^\star_{f'}}(\xi)\ \mathrm{d}^2\xi_A}{\iint \iint \sum_f \sum_{f'} \gamma''_f \gamma^\star_{f'} K_{\Theta''_f}(\xi) K_{\Theta^\star_{f'}}(\xi)\ \mathrm{d}^2\xi_A\ \mathrm{d}^2\xi_S}$$

$$= \frac{\sum_f \sum_{f'} \gamma''_f \gamma^\star_{f'} \iint K_{\Xi_{ff'}}(\xi)\ \mathrm{d}^2\xi_A}{\sum_f \sum_{f'} \gamma''_f \gamma^\star_{f'} \iint \iint K_{\Xi_{ff'}}(\xi)\ \mathrm{d}^2\xi_A\ \mathrm{d}^2\xi_S} \tag{III.42}$$

$$= (2\pi)^{-1} \frac{\sum_f \sum_{f'} \frac{\gamma''_f \gamma^\star_{f'}}{\sqrt{\det \lfloor \Xi_{ff'} \rceil_A}} K_{\Xi'_{ff'}}(\xi_S)}{\sum_f \sum_{f'} \frac{\gamma''_f \gamma^\star_{f'}}{\sqrt{\det \Xi_{ff'}}}} \ .$$

The relations (III.40) and (III.42) apply to both the positive ($\bullet$) and the negative ($\circ$) outcomes.

C Embracing displaced states

So far we have described the subtraction procedure in terms of linear combinations of Gaussian kernels. This description permits subtraction from multiple modes of a multipartite system. Unfortunately no matter how versatile this decomposition seems to be so far, it does not cover displaced states. This lack of compatibility follows the initial presumption of zero vectors of mean values.

The inclusion of displaced states essentially boils down to three problems. First we must extend the description of linear transformations (induced by Gaussian operations). Second the product of two displaced Gaussian kernels must be found and finally, the integral transformation has to be taken into account.

The problem with linear transformations was addressed in (III.20) and (III.23). Under the assumption of orthogonal transformations the characteristic matrix of a Gaussian kernel transforms the same way the regular variance matrix would. The same applies to the vector of mean values, the transformations reading

$$\Theta \mapsto V\Theta V^\intercal \ , \quad \mu \mapsto V\mu \ . \tag{III.43}$$

In order to address the second problem, consider a displaced Gaussian kernel

$$K_{\mu\Theta}(\xi) = \exp\left(-\frac{1}{2}(\xi-\mu)^{\intercal}\Theta(\xi-\mu)\right) , \tag{III.44}$$

where the vector of mean values μ defines the displacement and Θ denotes the respective characteristic matrix. Suppose there is a product

$$K_{\mu\Theta}(\xi)K_{\nu\Omega}(\xi) \tag{III.45}$$

of two Gaussian kernels (III.44), the first one characterized by the (μ,Θ) pair and the other one by the pair (ν,Ω). We are going to show that the product relation

$$K_{\mu\Theta}(\xi)K_{\nu\Omega}(\xi) = \exp\left(-\frac{1}{2}\zeta\right) K_{\delta\Xi}(\xi) \tag{III.46}$$

holds for all Gaussian kernels satisfying that at least one of the matrices is invertible. The Gaussian kernel and the factor on the right hand side of (III.46) comprise

$$\begin{aligned} \Xi &= \Theta + \Omega \\ \Delta &= \Theta\mu + \Omega\nu \\ \delta &= \Xi^{-1}\Delta \\ \zeta &= \mu^{\intercal}\Theta\mu + \nu^{\intercal}\Omega\nu - \Delta^{\intercal}\Xi^{-1}\Delta \, . \end{aligned} \tag{III.47}$$

We may therefore extend the product relation (III.24) to account for more general Wigner functions decomposing into these generalised Gaussian kernels. Their product then reads

$$\begin{aligned} W_{\hat{\varrho}}(\xi)W_{\hat{\Pi}}(\xi) &= \sum_{f}\sum_{f'} \gamma_f \vartheta_{f'} K_{\mu_f\Theta_f}(\xi)K_{\nu_{f'}\Omega_{f'}}(\xi) \\ &= \sum_{f}\sum_{f'} \gamma_f \vartheta_{f'} \exp\left(-\frac{1}{2}\zeta_{ff'}\right) K_{\delta_{ff'}\Xi_{ff'}}(\xi) \end{aligned} \tag{III.48}$$

with the ff' components obtained using the relations (III.46) and (III.47). The expressions in (III.47) become clear if we expand the left hand side of (III.46). The

product of the two Gaussian kernels gives a sum of their respective quadratic forms,

$$\begin{aligned}(\xi-\mu)^\intercal\Theta(\xi-\mu)+(\xi-\nu)^\intercal\Omega(\xi-\nu)=\\ \xi^\intercal\Theta\xi-\xi^\intercal\Theta\mu-\mu^\intercal\Theta\xi+\mu^\intercal\Theta\mu+\xi^\intercal\Omega\xi-\xi^\intercal\Omega\nu-\nu^\intercal\Omega\xi+\nu^\intercal\Omega\nu=\\ \xi^\intercal\underbrace{(\Theta+\Omega)}_{\Xi}\xi-2\xi^\intercal\underbrace{(\Theta\mu+\Omega\mu)}_{\Delta}+\mu^\intercal\Theta\mu+\nu^\intercal\Omega\nu\ .\end{aligned} \tag{III.49}$$

Where we have exploited that the matrices Θ and Ω are symmetrical. Consider an arbitrary Gaussian kernel characterized by (δ,Ξ) with symmetrical Ξ. The expansion of its quadratic form

$$\begin{aligned}(\xi-\delta)^\intercal\Xi(\xi-\delta)&=\xi^\intercal\Xi\xi-\xi^\intercal\Xi\delta-\delta^\intercal\Xi\xi+\delta^\intercal\Xi\delta\\ &=\xi^\intercal\Xi\xi-2\xi^\intercal(\Xi\delta)+\delta^\intercal\Xi\delta\end{aligned} \tag{III.50}$$

may be compared to right hand side of (III.49). We may notice the striking similarities in the second terms of both expressions, yielding

$$\begin{aligned}\xi^\intercal\Delta=\xi^\intercal(\Xi\delta)\implies\Delta=\Xi\delta\\ \implies\delta=\Xi^{-1}\Delta\ .\end{aligned} \tag{III.51}$$

It is therefore possible to express the right hand side of (III.49) using a single quadratic expression and a constant additive factor

$$\begin{aligned}\xi^\intercal\Xi\xi-2\xi^\intercal\Delta+\mu^\intercal\Theta\mu+\nu^\intercal\Omega\nu=\\ (\xi-\delta)^\intercal\Xi(\xi-\delta)+\underbrace{\mu^\intercal\Theta\mu+\nu^\intercal\Omega\nu-\delta^\intercal\Xi\delta}_{\zeta}\ .\end{aligned} \tag{III.52}$$

This result allows us to reuse some of the old tricks in our hat and resolve the third problem. The integral induced transformation (III.27) of the kernel product (III.46) becomes rather straightforward

$$\exp\left(-\frac{1}{2}\zeta\right)\int K_{\delta\Xi}(\xi)\ \mathrm{d}\xi_f\ , \tag{III.53}$$

where the substitution $\tau=\xi-\delta$ gives the well known integral transformation (III.28)

$$\int K_\Xi(\tau)\ \mathrm{d}\tau_f\mapsto\sqrt{\frac{2\pi}{\Xi_{ff}}}K_{\Xi'}(\tau)\ . \tag{III.54}$$

This integral map has to be treated the same way as the one obtained earlier in (III.28) to resolve the potential formal issues. The transformed Gaussian kernel (III.46) accompanied by the all the multiplicative factors reads

$$\exp\left(-\frac{1}{2}\zeta\right) K_{\delta\Xi'}(\tau)\sqrt{\frac{2\pi}{\Xi_{ff}}} \tag{III.55}$$

with the inverse substitution $\tau = \xi - \delta$ putting δ back into the play, yielding the

$$\exp\left(-\frac{1}{2}\zeta\right)\int K_{\delta\Xi}\left(\xi\right)\,\mathrm{d}\xi_f \mapsto \exp\left(-\frac{1}{2}\zeta\right)\sqrt{\frac{2\pi}{\Xi_{ff}}}K_{\delta\Xi'}\left(\xi\right)\,, \tag{III.56}$$

implying the vector of mean values δ is invariant in respect to the integral transformation. This method may be effortlessly repeated again to obtain the planar integral (III.35) over the χth mode

$$\exp\left(-\frac{1}{2}\zeta\right)\int K_{\delta\Xi}\left(\xi\right)\,\mathrm{d}^2\xi_\chi \mapsto \exp\left(-\frac{1}{2}\zeta\right)\frac{2\pi}{\sqrt{\det\lfloor\Theta\rceil_\chi}}K_{\delta\Xi'}\left(\xi\right) \tag{III.57}$$

with the transformed characteristic matrix Ξ defined by the relation (III.34) and the symbol $\lfloor\Theta\rceil_\chi$ denoting the 2×2 submatrix respective to the χth mode.

We have therefore obtained a decomposition of a Wigner function into general Gaussian kernels defined by (III.44)

$$W(\xi) = \sum_f \gamma_f K_{\mu_f\Theta_f}(\xi)\,. \tag{III.58}$$

In this general formulation the subtraction procedure outlined in the subsection III.2.B requires only some minor changes in each part of the procedure.

(1) The non-zero vectors μ_f^S of mean values of the signal state have to be taken into account, the joint vector

$$\mu_f = \mu_f^S \oplus (0,0)^\intercal \oplus (0,0)^\intercal \tag{III.59}$$

given by the direct matrix product of the individual vectors. The equivalent

to the Wigner function (III.15) reads

$$W_{SAL}(\xi) = \sum_f \gamma_f K_{\mu_f \Theta_f}(\xi) \ , \tag{III.60}$$

where the γ_f factors and Θ_f matrices follow the relations accompanying (III.15).

(2) The analogue of the transformed Wigner function (III.21) reads

$$W'_{SAL}(\xi) = \sum_f \gamma_f K_{\mu'_f \Theta'_f}(\xi) \tag{III.61}$$

with the joint vector of mean values transformed by the interaction into

$$\mu_f \mapsto \mu'_f = V \mu_f \ . \tag{III.62}$$

(3) The components of the product state now obey the relation (III.46) instead of the formula (III.25). The marginal Wigner function (III.36) therefore becomes

$$W_{SA}(\xi) = \sum_f \gamma_f \frac{2\pi}{\det \lfloor \Theta'_f \rceil_L} K_{\mu'_f \Theta''_f}(\xi) = \sum_f \gamma''_f K_{\mu'_f \Theta''_f}(\xi) \tag{III.63}$$

where the cumulative factors γ''_f comprise

$$\gamma''_f = \gamma_f \frac{2\pi}{\det \lfloor \Theta'_f \rceil_L} \ . \tag{III.64}$$

(4) The relation (III.42) describing the resulting state now incorporates the vector of mean values as well, the product of the underlying Gaussian kernels now obeys the relation (III.46), the final Wigner function consequently reads

$$W^{\bigstar}(\xi_S) = (2\pi)^{-1} \frac{\sum_f \sum_{f'} \frac{\gamma''_f \gamma^{\bigstar}_{f'}}{\sqrt{\det \lfloor \Xi_{ff'} \rceil_A}} \exp\left(-\frac{1}{2}\zeta_{ff'}\right) K_{\delta_{ff'} \Xi'_{ff'}}(\xi_S)}{\sum_f \sum_{f'} \frac{\gamma''_f \gamma^{\bigstar}_{f'}}{\sqrt{\det \Xi_{ff'}}} \exp\left(-\frac{1}{2}\zeta_{ff'}\right)} \tag{III.65}$$

with the factors γ''_f coming from (III.64) and $\gamma^{\bigstar}_{f'}$ from (III.39). The joint characteristic matrices Ξ_{ff}, the joint vectors of mean values $\delta_{ff'}$ and the additional factors $\exp\left(-\frac{1}{2}\zeta_{ff'}\right)$ are governed by the product relation (III.46),

starting with the individual matrices and vectors of (III.63) and (III.39). Furthermore the characteristic matrices $\Xi'_{ff'}$ result from the subsequent planar integral (III.57).

Consequently the probability relation associated with (III.65) reads

$$P^{\bigstar} = (2\pi)^3 \sum_{f} \sum_{f'} \frac{\gamma''_f \gamma^{\bigstar}_{f'}}{\sqrt{\det \Xi_{ff'}}} \exp\left(-\frac{1}{2}\zeta_{ff'}\right) . \tag{III.66}$$

3 Improved subtraction procedure revisited

In the previous sections we demonstrated the insufficiency of a description based solely on Gaussian Wigner functions and introduced an approach aiming to resolve its shortcomings without straying too far from the Gaussian nature of the description. We focused on the analysis of the original subtraction procedure, a building block of the improved version of the protocol.

Our efforts bore fruit and we developed a decomposition (III.58) of a Wigner function into general Gaussian kernels defined by the relation (III.44) and most importantly demonstrated the effects of the original subtraction protocol on this class of states. It is clear from the formulae (III.58) and (III.65) that the set of states described by Wigner functions that may be decomposed into arbitrarily displaced Gaussian kernels (III.58) is closed in respect to the original subtraction procedure.

The Wigner function (II.18) describing the state after the successful execution of the improved subtraction procedure is a weighted linear combination of Wigner functions, which are in essence given by repeated application of the formula (III.65) as each $W_f(\xi)$ in (II.18) describes an individual chain (*cf.* Figure II.3) of the original subtraction procedures.

In each iterative chain the original subtraction procedure is repeated until it finally succeeds (*cf.* Figure II.2) and the respective Wigner function $W_f(\xi)$ of the resulting state is given by the general relation (III.65) where $\bigstar = \bullet$ denotes a successful subtraction. The elements of the intermediate input state (III.58) in this final iteration f are given by the very same relation (III.65) with $\bigstar = \circ$ standing for an unsuccessful subtraction attempt in the preceding iteration $(f-1)$. The elements

in each prior iteration $(f-1)\ldots 1$ are obtained in the same fashion.

The Wigner functions $W_f(\xi)$ describing the iterative chains can be decomposed into (III.58) again and the set of Wigner functions (III.58) is therefore closed in respect to the chain of subtraction attempts and consequently so is the improved subtraction procedure (II.18).

Chapter IV

Superposed coherent states

Quantum superposition is one of the fundamental principles of quantum physics and consequently states in quantum superposition play a vital role in many applications including the quantum information theory. It is therefore only appropriate to explore how well the improved subtraction procedure preserves quantum superpositions. We make use of superposed coherent (Schrödinger cat) states in our subsequent investigation of the subtraction procedure due to their relative fragility.

The Schrödinger cat states in quantum optics are defined as coherent superpositions of two coherent states with opposite phases [29], their definition permitting two distinct types of such states in general

$$|\Psi_{\pm}\rangle = \frac{|\alpha\rangle \pm |-\alpha\rangle}{2 \pm 2\exp(-2|\alpha|^2)} \,. \tag{IV.1}$$

The $|\Psi_{+}\rangle$ is called the **even cat state** as it only comprises even number states, while the **odd cat state** $|\Psi_{-}\rangle$ is composed solely of odd number states.

The transition between the two cat states $|\Psi_{+}\rangle$ and $|\Psi_{-}\rangle$ may be facilitated using the annihilation operator $\hat{a}$. This may be immediately seen from the definition (I.41) of a coherent state. The improved subtraction procedure is essentially an approximation of the annihilation operator and the ideal transition relation $|\Psi_{\pm}\rangle \rightleftharpoons |\Psi_{\mp}\rangle$ may be therefore exploited to quantify the preservation of quantum superpositions.

Suppose the subtraction procedure is applied to one of the cat states. In the ideal case the transformed state should be identical to the other cat state. The difference

between the expected and the acquired states can be measured in the usual way using fidelity [20, 22]. Suppose the Wigner function of the expected state reads $W_{\pm}(x,p)$ and the acquired state is described with $W(x,p)$. The fidelity of the process reads

$$F_{\pm} = 2\pi \iint W(x,p) W_{\pm}(x,p) \, \mathrm{d}x \, \mathrm{d}p \, . \tag{IV.2}$$

In the following paragraphs we are going to derive the Wigner functions $W_{\pm}(x,p)$ of both the coherent cat states (IV.1) in a formulation compatible with the decomposition developed in the chapter III and analyse the fidelity of the transformation $W_{+}(x,p) \to W_{-}(x,p)$ facilitated by the improved subtraction procedure (chapter II).

1 Coherent cat states in phase space representation

We are interested in the Wigner functions $W_{\pm}(x,p)$ respective to both the even and odd cat states $|\Psi_{\pm}\rangle$. Starting with the transformation formula (I.8) we obtain

$$\begin{aligned}
W_{\pm}(x,p) &= \pi^{-1} \int \exp(2\imath p\zeta) \, \langle x-\zeta \,|\, \Psi_{\pm} \rangle \, \langle \Psi_{\pm} \,|\, x+\zeta \rangle \, \mathrm{d}\zeta \\
&= \frac{\pi^{-1}}{2 \pm 2\exp(-2|\alpha|^2)} \times \\
&\quad \int \exp(2\imath p\zeta) \Big(\langle x-\zeta \,|\, \alpha \rangle \pm \langle x-\zeta \,|\, -\alpha \rangle \Big) \times \\
&\qquad\qquad \Big(\langle \alpha \,|\, x+\zeta \rangle \pm \langle -\alpha \,|\, x+\zeta \rangle \Big) \, \mathrm{d}\zeta \\
&= \frac{\pi^{-1}}{2 \pm 2\exp(-2|\alpha|^2)} \times \\
&\quad \int \exp(2\imath p\zeta) \Big(f_{\alpha}(x-\zeta) \pm f_{-\alpha}(x-\zeta) \Big) \times \\
&\qquad\qquad \Big(\bar{f}_{\alpha}(x+\zeta) \pm \bar{f}_{-\alpha}(x+\zeta) \Big) \, \mathrm{d}\zeta \, ,
\end{aligned} \tag{IV.3}$$

where the $f_{\pm\alpha}(x \pm \zeta) = \langle x \pm \zeta \,|\, \pm\alpha \rangle$ wave functions and their complex conjugates follow the defining relation (I.46). The expansion of the product reads

$$
\begin{aligned}
W_{\pm}(x,p) = \frac{\pi^{-1}}{2 \pm 2\exp(-2|\alpha|^2)} \times \Bigg(& \\
& \int \exp(2\imath p\zeta) \underbrace{f_{\alpha}(x-\zeta)\bar{f}_{\alpha}(x-\zeta)}_{①} \,\mathrm{d}\zeta \pm \\
& \int \exp(2\imath p\zeta) \underbrace{f_{\alpha}(x-\zeta)\bar{f}_{-\alpha}(x+\zeta)}_{②} \,\mathrm{d}\zeta \pm \\
& \int \exp(2\imath p\zeta) \underbrace{f_{-\alpha}(x-\zeta)\bar{f}_{\alpha}(x+\zeta)}_{③} \,\mathrm{d}\zeta + \\
& \int \exp(2\imath p\zeta) \underbrace{f_{-\alpha}(x-\zeta)\bar{f}_{-\alpha}(x+\zeta)}_{④} \,\mathrm{d}\zeta \Bigg)
\end{aligned}
\tag{IV.4}
$$

with the individual (numbered) elements of the product comprising the wave functions (I.46). After some algebra the elements are obtained in the form

$$
\begin{aligned}
① &= \frac{1}{\sqrt{\pi}} \exp\left[-(x-x_0)^2\right] \exp\left[-\zeta^2 - 2\imath p_0\zeta\right] \\
② &= \frac{1}{\sqrt{\pi}} \exp\left[-(x-\imath p_0)^2\right] \exp\left[-(\zeta+x_0)^2\right] \exp\left[-p_0^2\right] \\
③ &= \frac{1}{\sqrt{\pi}} \exp\left[-(x+\imath p_0)^2\right] \exp\left[-(\zeta-x_0)^2\right] \exp\left[-p_0^2\right] \\
④ &= \frac{1}{\sqrt{\pi}} \exp\left[-(x+x_0)^2\right] \exp\left[-\zeta^2 + 2\imath p_0\zeta\right] \ ,
\end{aligned}
\tag{IV.5}
$$

their subsequent integral transformations inevitably yielding the components

$$\begin{aligned}
\int \exp(2\imath p\zeta)\,\textcircled{1}\,\mathrm{d}\zeta &= \exp\left[-(x-x_0)^2-(p-p_0)^2\right]\\
\int \exp(2\imath p\zeta)\,\textcircled{2}\,\mathrm{d}\zeta &= \exp\left[-(x-\imath p_0)^2-(p+\imath x_0)^2\right]\exp\left[-2|\alpha|^2\right]\\
\int \exp(2\imath p\zeta)\,\textcircled{3}\,\mathrm{d}\zeta &= \exp\left[-(x+\imath p_0)^2-(p-\imath x_0)^2\right]\exp\left[-2|\alpha|^2\right]\\
\int \exp(2\imath p\zeta)\,\textcircled{4}\,\mathrm{d}\zeta &= \exp\left[-(x+x_0)^2-(p+p_0)^2\right]
\end{aligned} \tag{IV.6}$$

of the respective Wigner functions of both the even and odd cat states

$$\begin{aligned}
W_{\pm}(x,p) = \frac{\pi^{-1}}{2\pm 2\exp(-2|\alpha|^2)} \times \Big\{ & \\
& \exp\left[-(x-x_0)^2-(p-p_0)^2\right] \pm \\
& \exp\left[-(x-\imath p_0)^2-(p+\imath x_0)^2\right]\exp\left[-2|\alpha|^2\right] \pm \\
& \exp\left[-(x+\imath p_0)^2-(p-\imath x_0)^2\right]\exp\left[-2|\alpha|^2\right] + \\
& \exp\left[-(x+x_0)^2-(p+p_0)^2\right] \\
\Big\}\,. &
\end{aligned} \tag{IV.7}$$

The Wigner functions (IV.7) seem to be ill defined as their ranges appear to be complex. Fortunately the two complex components add up in a way that eliminates their complex nature, yielding a modulated harmonic interference pattern [30].

Furthermore the Wigner functions (IV.7) may be directly decomposed into a set of four Gaussian kernels with different weights and different displacement vectors

$$\begin{aligned}
\gamma_1^S &= \gamma\,, & \mu_1^S &= (x_0,p_0)^{\intercal}\,, & \Theta_1^S &= \Theta\\
\gamma_2^S &= \pm\exp\left[-2|\alpha|^2\right]\gamma\,, & \mu_2^S &= (\imath p_0,-\imath x_0)^{\intercal}\,, & \Theta_2^S &= \Theta\\
\gamma_3^S &= \pm\exp\left[-2|\alpha|^2\right]\gamma\,, & \mu_3^S &= (-\imath p_0,\imath x_0)^{\intercal}\,, & \Theta_3^S &= \Theta\\
\gamma_4^S &= \gamma\,, & \mu_4^S &= (-x_0,-p_0)^{\intercal}\,, & \Theta_4^S &= \Theta
\end{aligned} \tag{IV.8}$$

where the common factor γ and the common characteristic matrix Θ read

$$\gamma = \frac{\pi^{-1}}{2\pm 2\exp(-2|\alpha|^2)}\,, \quad \Theta = \mathrm{diag}(2,2)\,. \tag{IV.9}$$

2 Quantification of superposition preservation

The preservation of quantum superpositions by the improved subtraction procedure is quantified using the fidelity of the transition

$$W_+(x,p) \to W_-(x,p) \; . \tag{IV.10}$$

We start with the signal Wigner function $W_S(x,p) = W_+(x,p)$ decomposed into

$$W_S(x,p) = W_+(x,p) = \sum_{f=1}^{4} \gamma_f^S K_{\mu_f^S \Theta_f^S}(x,p) \tag{IV.11}$$

with γ_f^S, μ_f^S and Θ_f^S given by the values (IV.8). This Wigner function is then transformed by the improved subtraction procedure into (II.18). The result may be decomposed into (III.58), the final linear combination reading

$$W_N(x,p) = \sum_{f}^{8\times N} \gamma_f K_{\mu_f \Theta f}(x,p) \; . \tag{IV.12}$$

where N denotes the **maximal number of iterations** under consideration. The fidelity (IV.2) of the transition is then given by the overlap integral

$$F_N = 2\pi \iint W_N(x,p) W_-(x,p) \; \mathrm{d}x \; \mathrm{d}p \tag{IV.13}$$

which may be evaluated in a straightforward fashion with the aid of the product formula (III.48) and the integral formulae (III.56), and (III.35).

The fidelity is computed numerically for the signal state $W_+(x,p)$. The computation is evaluated for different settings of the improved procedure, i.e., for different numbers N of iterations, different transmittances ζ and detection efficiencies η.

The implicit mapping between the overall success probability Q (II.17) and the fidelity F (IV.2) of the transition $W_+(x,p) \to W_-(x,p)$ is shown in the Figure IV.1. The curves are obtained by varying the transmittance ζ and plotting the respective values of probability and fidelity. Each curve is associated with a different number of iterations N and detection efficiency η.

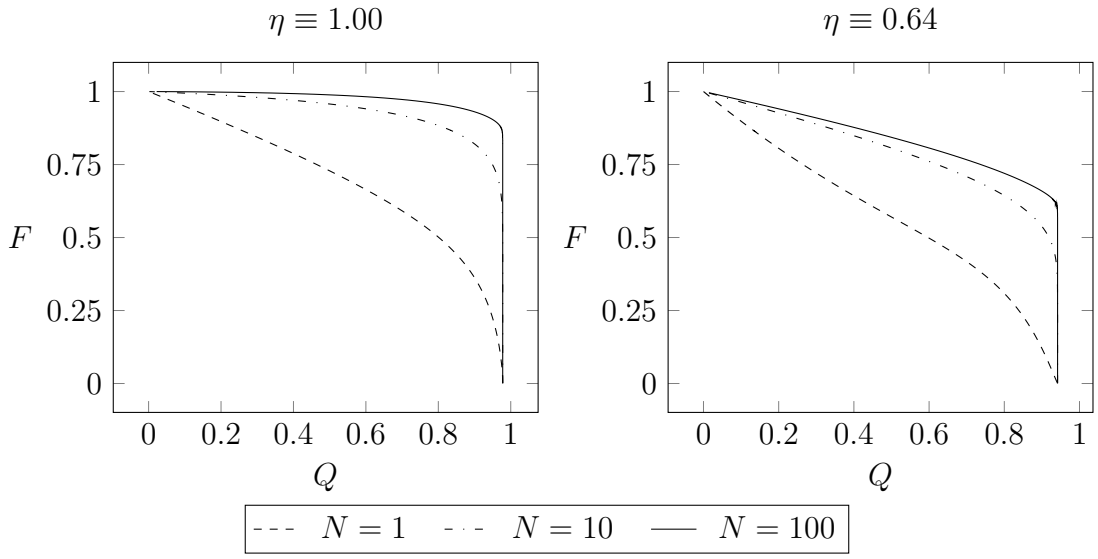

Figure IV.1: The overall probability — fidelity mappings are obtained for the subtraction procedure employing an ideal avalanche photodiode (efficiency $\eta \equiv 1$, on the left) and a realistic, inefficient photodiode ($\eta \equiv 0.64$, on the right). Both the plots are computed for the transition between coherent cat states with complex amplitudes (I.43) given as $\alpha_{\pm} = \pm\frac{3}{\sqrt{2}}$.

The higher fidelities of the $W_+(x,p) \to W_-(x,p)$ transition are obtained with negligible probabilities for the original procedure ($N = 1$) which is, in comparison, clearly outperformed by the improved procedure ($N \geq 2$).

Consider for example the ideal case (on left). Fixing the fidelity $F \approx 0.92$, the respective probabilities read $Q_{N=1} \approx 0.15$ and $Q_{N=100} \approx 0.92$, the latter probability roughly six times larger. A similar comparison can be made for the realistic case.

The improved subtraction procedure outperforms the original subtraction protocol in terms of the transition fidelity, i.e., in terms of preservation of quantum superposition of coherent states. The performance of the improved procedure increases with the maximal number of iterations (subtraction attempts) in consideration as can be immediately seen from the Figure IV.1. The first few iterations are most significant in both the ideal and the inefficient detection regimes. The inefficiency of the detection negatively impacts the attainable fidelity of the transition. This can be suppressed but not surpassed with a higher number of subtraction attempts, ultimately making an efficient ($\eta \to 1$) detection a necessary requirement.

Chapter V

Entanglement distillation

The notion of quantum entanglement [25] was originally introduced long before the advent of the quantum information theory and quantum cryptography (quantum key distribution). It is now a crucial ingredient of both [4, 6, 20, 21, 31, 32]. Entangled states are susceptible to decoherence, resulting in decay and eventual loss of their entanglement [33, 34]. This fragility is a particularly significant obstacle in quantum communication utilizing lossy channels over long distances [35, 36]. The decay of entanglement may be suppressed with entanglement purification strategies employing local operations and classical communication to increase the mutual entanglement using either single or multiple copies of the insufficiently entangled states [4, 6, 37]. It was proven that it is fundamentally impossible to distil entanglement from any number of copies of a bipartite Gaussian state using only Gaussian operations and classical communication [8, 9, 10]. Since the quantum optical realizations of concepts of the continuous variable information theory such as quantum teleportation [38, 39] and quantum key distribution [32, 40, 41, 42] utilize Gaussian operations and Gaussian two mode squeezed states, the search for alternative methods of entanglement distillation becomes necessary.

One such method in particular exploits subtraction of a single photon [15]. The method in question was originally introduced as a technique of conditionally improving the continuous variable teleportation and was subsequently implemented on various occasions in experimental setting [16, 17, 18]. In essence the subtraction procedure (described in the section II.1) was applied to both arms of an entangled two mode squeezed vacuum state. The entanglement distillation was considered

successful if both subtraction attempts were successful.

In this chapter we investigate the consequences of employing the improved photon subtraction procedure (introduced in section II.2) instead of the original one the distillation method was conceived with. In our present analysis the entanglement distillation procedure [15] is used to enhance entanglement in a single copy of a Gaussian two mode squeezed vacuum state.

Both the original and the improved subtraction procedures are employed in the distillation protocol and their effects are quantified using the Gaussian logarithmic negativity and EPR correlations (*cf.* section I.6). Furthermore the results are compared with an idealised realisation of the subtraction procedure directly employing the annihilation operators.

1 Idealised photon subtraction with annihilation operators

The entanglement measures in our consideration rely on variance matrices of quadrature operators of the entangled bipartite systems. In this section we obtain the analytical form of the variance matrix of quadrature operators of a two mode squeezed vacuum state transformed by the entanglement distillation procedure [15] employing the ideal single photon subtraction.

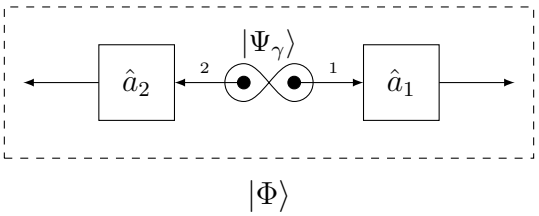

Figure V.1: A pair of annihilation operators is applied to the entangled two mode squeezed state $|\Psi_\gamma\rangle$, yielding the state $|\Phi\rangle$.

In the spirit of the distillation procedure presented in the Figure V.1 a pair of annihilation operators is applied to both arms of the bipartite signal state

$$|\Phi\rangle = \mathcal{N}\hat{a}_1\hat{a}_2\,|\Psi_\gamma\rangle \ , \tag{V.1}$$

where $|\Psi_\gamma\rangle$ represents the two mode squeezed state (I.50)—(I.51). Because neither operator preserves normalisation, the resulting state has to be renormalised. Following the standard interpretation of quantum mechanics the normalisation reads

$$\mathcal{N} = \frac{1}{\sqrt{\langle\Psi_\gamma|\hat{a}_2^\dagger\hat{a}_1^\dagger\hat{a}_2\hat{a}_1|\Psi_\gamma\rangle}} = \frac{1}{\sqrt{\langle\Psi_\gamma|\hat{n}_1\hat{n}_2|\Psi_\gamma\rangle}} \,, \tag{V.2}$$

where the commutation relations (I.5) permit the reordering of the creation and annihilation operators, yielding the respective number operators

$$\hat{n}_f = \hat{a}_f^\dagger\hat{a}_f \qquad \forall f = 1, 2 \,. \tag{V.3}$$

We may obtain the exact value of the normalisation factor $\mathcal{N}$ by expanding the two mode squeezed vacuum state (I.50) in the number representation. The expectation value in the denominator of the relation (V.2) becomes

$$\begin{aligned}
\langle\Psi_\gamma|\hat{n}_1\hat{n}_2|\Psi_\gamma\rangle &= (1-\lambda^2)\sum_{f'}\sum_{f}\lambda^f\lambda^{f'}\,\langle f'|\hat{n}_1|f\rangle\,\langle f'|\hat{n}_2|f\rangle \\
&= (1-\lambda^2)\sum_{f'}\sum_{f}\lambda^f\lambda^{f'}\delta_{ff'}\delta_{ff'}f^2 \\
&= (1-\lambda^2)\sum_{f}\lambda^{2f}f^2
\end{aligned} \tag{V.4}$$

with $\lambda = \tanh\gamma$ following the relation (I.50). The summation on the right hand side converges for $|\lambda| < 1$ and its value may be found in the closed-form (A.3). Finally an explicit formula for the normalisation factor is found

$$\mathcal{N} = \frac{1-\lambda^2}{\lambda\sqrt{1+\lambda^2}} \,, \tag{V.5}$$

which may be substituted back into the original expression (V.1) for the subtracted two mode squeezed state. Using the expansion (I.50) for $|\Psi_\gamma\rangle$ again, we readily

obtain the state in the number representation

$$\begin{aligned}
|\Phi\rangle &= \mathcal{N}\hat{a}_1\hat{a}_2\,|\Psi_\gamma\rangle \\
&= \mathcal{N}\sqrt{1-\lambda^2}\sum_f \lambda^f f\,|f-1\rangle\,|f-1\rangle \\
&= \mathcal{N}\sqrt{1-\lambda^2}\sum_f \lambda^{f+1}(f+1)\,|f\rangle\,|f\rangle \\
&= \sum_f \vartheta_f\,|f\rangle\,|f\rangle\ ,
\end{aligned} \tag{V.6}$$

where the cumulative weights ϑ_f in the summation consequently read

$$\begin{aligned}
\vartheta_f &= \mathcal{N}\sqrt{1-\lambda^2}\lambda^{f+1}(f+1) \\
&= \frac{1-\lambda^2}{\lambda\sqrt{1+\lambda^2}}\sqrt{1-\lambda^2}\lambda^{f+1}(f+1) \\
&= \sqrt{\frac{(1-\lambda^2)^3}{1+\lambda^2}}\lambda^f(f+1)\ .
\end{aligned} \tag{V.7}$$

We are now in a perfect position to derive the variance matrix of the quadrature operators of the state (V.6). Consider a vector of the quadrature operators (I.6) of both arms of the entangled system first

$$\hat{\xi} = (\hat{x}_1, \hat{p}_1, \hat{x}_2, \hat{p}_2)^\intercal\ . \tag{V.8}$$

The elements σ_{ij} of the respective 4×4 variance matrix σ are given by the formula

$$\sigma_{ij} = \frac{1}{2}\langle\hat{\xi}_i\hat{\xi}_j + \hat{\xi}_j\hat{\xi}_i\rangle - \langle\hat{\xi}_i\rangle\langle\hat{\xi}_j\rangle \qquad \forall i,j = 1\ldots 4\ , \tag{V.9}$$

where the first quadratic (symmetrical) expression reflects the general lack of commutativity of the operators in question.

Because the state (V.6) is defined in the number representation it is convenient to restate the quadrature operators in terms of the creation and annihilation operators of the optical field. Consequently the elements of the variance matrix σ comprise expectation values of the field operators and their quadratic products.

With some effort we may show that the expectation values linear in the field oper-

ators simply vanish. Consider the annihilation operator $\hat{a}_l$ of either mode

$$\begin{aligned}\langle \hat{a}_l \rangle &= \sum_{f'} \sum_{f} \vartheta_{f'} \vartheta_f \langle f' | \hat{a}_l | f \rangle \langle f' | f \rangle \\ &= \sum_{f'} \sum_{f} \vartheta_{f'} \vartheta_f \sqrt{f} \langle f' | f-1 \rangle \langle f' | f \rangle \ ,\end{aligned} \tag{V.10}$$

where the inner products on the right hand side lead to a pair of conflicting conditions $(f = f' - 1) \wedge (f = f')$ which may never be satisfied simultaneously. A similar conflict occurs in the case of the expectation value of the conjugate operators $\langle \hat{a}_l^\dagger \rangle$. As a consequence the expectation values at hand cancel out completely

$$\langle \hat{a}_l \rangle = \langle \hat{a}_l^\dagger \rangle = 0 \qquad \forall l = 1, 2 \ . \tag{V.11}$$

Following the definition (I.6) we obtain the same results for the quadrature operators,

$$\langle \hat{x}_l \rangle = \langle \hat{p}_l \rangle = 0 \qquad \forall l = 1, 2 \ . \tag{V.12}$$

Turning our attention to the quadratic products of the field operators we can show that some of the expectation values vanish as well. Consider the operators acting on the same modes first. Their expectation values

$$\langle \hat{a}_1 \hat{a}_1 \rangle = \langle \hat{a}_2 \hat{a}_2 \rangle = \langle \hat{a}_1^\dagger \hat{a}_1^\dagger \rangle = \langle \hat{a}_2^\dagger \hat{a}_2^\dagger \rangle \tag{V.13}$$

are identical since the structure of the state is symmetrical in both modes. Similarly the mixed quadratic products involving annihilation in one mode and creation in the other give identical results $\langle \hat{a}_1 \hat{a}_2^\dagger \rangle = \langle \hat{a}_1^\dagger \hat{a}_2 \rangle$. It is therefore necessary to only consider the following pair of relations

$$\begin{aligned}\langle \hat{a}_1 \hat{a}_1 \rangle &= \sum_{f'} \sum_{f} \vartheta_{f'} \vartheta_f \langle f' | \hat{a}_1 \hat{a}_1 | f \rangle \langle f' | f \rangle \\ &= \sum_{f'} \sum_{f} \vartheta_{f'} \vartheta_f \sqrt{f} \sqrt{f-1} \langle f' | f-2 \rangle \langle f' | f \rangle \ , \\ \langle \hat{a}_1 \hat{a}_2^\dagger \rangle &= \sum_{f'} \sum_{f} \vartheta_{f'} \vartheta_f \langle f' | \hat{a}_1 | f \rangle \langle f' | \hat{a}_2^\dagger | f \rangle \\ &= \sum_{f'} \sum_{f} \vartheta_{f'} \vartheta_f \sqrt{f} \sqrt{f'+1} \langle f'+1 | f-1 \rangle \langle f' | f \rangle \ ,\end{aligned} \tag{V.14}$$

which suffer from similar, impossible to satisfy, conditions. As a consequence the expectation values (V.14) cancel out completely

$$\langle \hat{a}_1 \hat{a}_1 \rangle = \langle \hat{a}_1^\dagger \hat{a}_1^\dagger \rangle = \langle \hat{a}_2 \hat{a}_2 \rangle = \langle \hat{a}_2^\dagger \hat{a}_2^\dagger \rangle = \langle \hat{a}_1 \hat{a}_2^\dagger \rangle = \langle \hat{a}_1^\dagger \hat{a}_2 \rangle = 0 \; . \tag{V.15}$$

The remaining quadratic products of the field operators lead to actual non-zero expectation values. Consider the expectation values of the number operators first

$$\begin{aligned} \langle \hat{a}_l^\dagger \hat{a}_l \rangle &= \sum_{f'} \sum_{f} \vartheta_{f'} \vartheta_f \, \langle f' | \hat{n}_l | f \rangle \, \langle f' | f \rangle \\ &= \sum_{f'} \sum_{f} \vartheta_{f'} \vartheta_f f \, \langle f' | f \rangle \, \langle f' | f \rangle \qquad \forall l = 1, 2 \; . \\ &= \sum_{f} \vartheta_f^2 f \end{aligned} \tag{V.16}$$

The expectation values of the reverse ordered quadratic products are acquired with the aid of the commutation relations (I.5), giving the values

$$\begin{aligned} \langle \hat{a}_l \hat{a}_l^\dagger \rangle &= \langle \hat{a}_l^\dagger \hat{a}_l + 1 \rangle \\ &= \sum_{f} \vartheta_f^2 f + 1 \qquad \forall l = 1, 2 \; . \end{aligned} \tag{V.17}$$

The final pair of the quadratic expectation values is obtained straightforwardly

$$\begin{aligned} \langle \hat{a}_1 \hat{a}_2 \rangle &= \sum_{f'} \sum_{f} \vartheta_{f'} \vartheta_f \, \langle f' | \hat{a}_1 | f \rangle \, \langle f' | \hat{a}_2 | f \rangle \\ &= \sum_{f'} \sum_{f} \vartheta_{f'} \vartheta_f f \, \langle f' | f - 1 \rangle \, \langle f' | f - 1 \rangle \\ &= \sum_{f} \vartheta_f \vartheta_{f+1} (f + 1) \; , \\ \langle \hat{a}_1^\dagger \hat{a}_2^\dagger \rangle &= \sum_{f'} \sum_{f} \vartheta_{f'} \vartheta_f \, \langle f' | \hat{a}_1^\dagger | f \rangle \, \langle f' | \hat{a}_2^\dagger | f \rangle \\ &= \sum_{f'} \sum_{f} \vartheta_{f'} \vartheta_f f' \, \langle f' - 1 | f \rangle \, \langle f' - 1 | f \rangle \\ &= \sum_{f} \vartheta_f \vartheta_{f+1} (f + 1) \; . \end{aligned} \tag{V.18}$$

We are now equipped with enough information to complete the variance matrix. As

we saw the expectation values linear in the quadrature operators vanish. Consequently the formula (V.9) yielding σ_{ij} elements simplifies into

$$\sigma_{ij} = \frac{1}{2}\langle \hat{\xi}_i \hat{\xi}_j + \hat{\xi}_j \hat{\xi}_i \rangle \ . \tag{V.19}$$

The commuting diagonal elements are evaluated with the aid of the relations (V.14), (V.16) and (V.17). We therefore obtain a quadruplet

$$\begin{aligned}
\sigma_{11} = \langle \hat{x}_1 \hat{x}_1 \rangle &= \frac{1}{2}\langle \hat{a}_1 \hat{a}_1^\dagger + \hat{a}_1^\dagger \hat{a}_1 + \hat{a}_1 \hat{a}_1 + \hat{a}_1^\dagger \hat{a}_1^\dagger \rangle &&= \frac{1}{2} + \langle \hat{n}_1 \rangle \ , \\
\sigma_{22} = \langle \hat{p}_1 \hat{p}_1 \rangle &= \frac{1}{2}\langle \hat{a}_1 \hat{a}_1^\dagger + \hat{a}_1^\dagger \hat{a}_1 - \hat{a}_1 \hat{a}_1 - \hat{a}_1^\dagger \hat{a}_1^\dagger \rangle &&= \frac{1}{2} + \langle \hat{n}_1 \rangle \ , \\
\sigma_{33} = \langle \hat{x}_2 \hat{x}_2 \rangle &= \frac{1}{2}\langle \hat{a}_2 \hat{a}_2^\dagger + \hat{a}_2^\dagger \hat{a}_2 + \hat{a}_2 \hat{a}_2 + \hat{a}_2^\dagger \hat{a}_2^\dagger \rangle &&= \frac{1}{2} + \langle \hat{n}_2 \rangle \ , \\
\sigma_{44} = \langle \hat{p}_2 \hat{p}_2 \rangle &= \frac{1}{2}\langle \hat{a}_2 \hat{a}_2^\dagger + \hat{a}_2^\dagger \hat{a}_2 - \hat{a}_2 \hat{a}_2 - \hat{a}_2^\dagger \hat{a}_2^\dagger \rangle &&= \frac{1}{2} + \langle \hat{n}_2 \rangle
\end{aligned} \tag{V.20}$$

of clearly identical values. Hence the diagonal of the variance matrix reads

$$\sigma_{ii} = \frac{1}{2} + \sum_f \vartheta_f^2 f \quad \forall\ i = 1 \ldots 4 \ . \tag{V.21}$$

The off-diagonal elements are derived in a similar fashion. Most of the correlations simply cancel out following the relation (V.15)

$$\begin{aligned}
\sigma_{12} = \sigma_{21} &= \frac{1}{2}\langle \hat{x}_1 \hat{p}_1 + \hat{p}_1 \hat{x}_1 \rangle = \frac{1}{2\imath}\langle \hat{a}_1 \hat{a}_1 + \hat{a}_1^\dagger \hat{a}_1^\dagger \rangle = 0 \ , \\
\sigma_{34} = \sigma_{43} &= \frac{1}{2}\langle \hat{x}_2 \hat{p}_2 + \hat{p}_2 \hat{x}_2 \rangle = \frac{1}{2\imath}\langle \hat{a}_2 \hat{a}_2 + \hat{a}_2^\dagger \hat{a}_2^\dagger \rangle = 0 \ , \\
\sigma_{14} = \sigma_{41} &= \frac{1}{2}\langle \hat{x}_1 \hat{p}_2 + \hat{p}_2 \hat{x}_1 \rangle = \frac{1}{2\imath}\langle \hat{a}_1 \hat{a}_2 - \hat{a}_1^\dagger \hat{a}_2^\dagger \rangle = 0 \ , \\
\sigma_{23} = \sigma_{32} &= \frac{1}{2}\langle \hat{x}_2 \hat{p}_1 + \hat{p}_1 \hat{x}_2 \rangle = \frac{1}{2\imath}\langle \hat{a}_1 \hat{a}_2 - \hat{a}_1^\dagger \hat{a}_2^\dagger \rangle = 0 \ .
\end{aligned} \tag{V.22}$$

Finally, the only non-zero off-diagonal elements of the variance matrix read

$$\begin{aligned}
\sigma_{13} = \sigma_{31} &= \frac{1}{2}\langle \hat{x}_1 \hat{x}_2 + \hat{x}_1 \hat{x}_2 \rangle &&= +\frac{1}{2}\langle \hat{a}_1 \hat{a}_2 + \hat{a}_1^\dagger \hat{a}_2^\dagger \rangle \ , \\
\sigma_{24} = \sigma_{42} &= \frac{1}{2}\langle \hat{p}_1 \hat{p}_2 + \hat{p}_1 \hat{p}_2 \rangle &&= -\frac{1}{2}\langle \hat{a}_1 \hat{a}_2 + \hat{a}_2^\dagger \hat{a}_2^\dagger \rangle \ .
\end{aligned} \tag{V.23}$$

It is clear that their absolute values are identical, given by the relation (V.18)

$$\sigma_{13} = \sigma_{31} = -\sigma_{24} = -\sigma_{42} = \sum_f \vartheta_f \vartheta_{f+1}(f+1) \; . \tag{V.24}$$

We can obtain explicit expressions for its the non-zero elements. The summation on the right hand side of (V.21) may be expanded into

$$\begin{aligned} \sum_f \vartheta_f^2 f &= \frac{(1-\beta)^3}{1+\beta} \sum_f \beta^f f(f+1)^2 \\ &= \frac{(1-\beta)^3}{1+\beta} \sum_f \beta^f (f + 2f^2 + f^3) \\ &= 2\frac{(1-\beta)^3}{1+\beta} \frac{\beta(2+\beta)}{(1-\beta)^4} \\ &= 2\frac{\beta(2+\beta)}{1-\beta^2} \; , \end{aligned} \tag{V.25}$$

where we set $\beta = \lambda^2 < 1$ and used the closed-form formulae (A.2), (A.3) and (A.4) derived in the appendix A. Similarly the summation in (V.23) becomes

$$\begin{aligned} \sum_f \vartheta_f \vartheta_{f+1}(f+1) &= \lambda \frac{(1-\beta)^3}{1+\beta} \sum_f \beta^f (f+2)(f+1)^2 \\ &= \lambda \frac{(1-\beta)^3}{1+\beta} \sum_f \beta^f (2 + 5f + 4f^2 + f^3) \\ &= 2\lambda \frac{(1-\beta)^3}{1+\beta} \frac{1+2\beta}{(1-\beta)^3} \\ &= 2\lambda \frac{1+2\beta}{1-\beta^2} \; . \end{aligned} \tag{V.26}$$

In conclusion the variance matrix of the quadrature operators reads

$$\sigma = \begin{pmatrix} \Delta & \cdot & \delta & \cdot \\ \cdot & \Delta & \cdot & -\delta \\ \delta & \cdot & \Delta & \cdot \\ \cdot & -\delta & \cdot & \Delta \end{pmatrix} \tag{V.27}$$

with Δ and δ given by the relations (V.21), (V.25), (V.23) and (V.26) as

$$\Delta = \frac{1}{2} + 2\frac{\beta(2+\beta)}{1-\beta^2} \ , \quad \delta = 2\lambda\frac{1+2\beta}{1-\beta^2} \ . \tag{V.28}$$

Clearly the variance matrix of the distilled state has the same structure as the input signal mode (I.52), however, its values have changed.

2 Subtraction with the improved subtraction procedure

In this section we investigate the consequences of employing the improved subtraction procedure in the entanglement distillation protocol. In the following paragraphs we adapt both subtraction procedures that were previously introduced in chapter II to accommodate the two mode signal state and to reflect its entangled nature. Subsequently we extend the conclusions of chapter III to provide a suitable description of the subtraction procedure in context of the entanglement distillation protocol.

The central idea of the improved subtraction procedure revolves around the way the unsuccessful subtraction attempts are handled. Because the original subtraction procedure is but a building block of the improved procedure we start with analysis of its necessary modifications first.

A basic scheme of the procedure is depicted in the Figure V.2. The principal difference (*cf.* Figure II.1b) lies in the number of the signal modes; the first signal mode S_I that does not take a part in the interaction directly is dashed out. Its physical properties are, however, affected due to its entanglement with the second, interacting mode S_{II}.

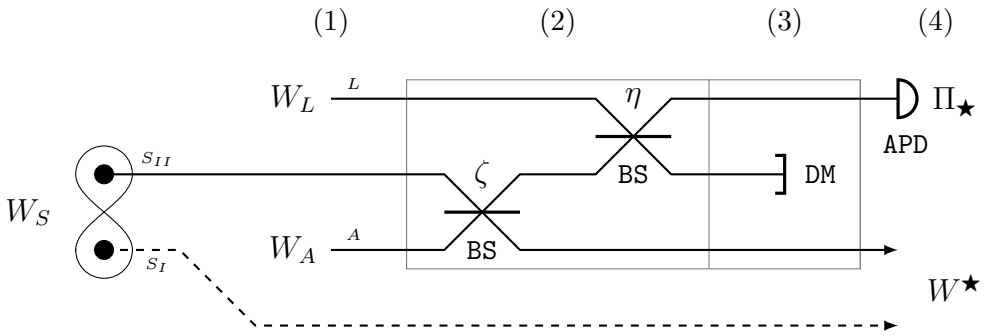

Figure V.2: The scheme is similar to the Figure II.1b with one difference. There is a pair of entangled signal modes present. Only one arm (S_{II}) directly participates in the interactions with the ancillary modes (A, L).

The interactions leading to the subtraction with outcome $\Pi_\bigstar$ (where $\bigstar \in \{\circ, \bullet\}$ denote the positive and negative outcomes, i.e., the successful and unsuccessful subtraction attempts) remain the same.

Similarly to the previous analysis (*cf.* Figure II.1b) the scheme of the procedure is divided into four logical units. We are going to describe each part of the scheme in the spirit of the analysis performed in chapter III and adapt the general formulation of subsection III.2.C to match the present circumstances.

(1) The input state comprises the entangled pair of signal modes and the factorized pair of idlers. Suppose the Wigner function $W_S(\xi_S)$ of the signal state is given in the form of a Gaussian decomposition (III.58) as

$$W_S(\xi_S) = \sum_f \gamma_f^S K_{\mu_f^S \Theta_f^S}(\xi_S) \tag{V.29}$$

with the 4×4 characteristic matrices Θ_f^S and the 4×1 vectors of mean values μ_f^S. In general these characteristic matrices may not be decomposed into a direct matrix sum due to the presence of correlations between the modes.

The Wigner function $W_{SAL}(\xi)$ of the joint state is then given by the familiar decomposition (III.60). The joint vector of phase space coordinates reads

$$\xi = \xi_S \oplus \xi_A \oplus \xi_L \tag{V.30}$$

with the vector ξ_S respective to the two mode signal state

$$\xi_S = (x_{S_I}, p_{S_I}, x_{S_{II}}, p_{S_{II}})^\intercal \ . \tag{V.31}$$

(2) The second mode (S_I) of the signal interacts with the idler (A) on a beam splitter of transmittance ζ. The idler then interacts with the virtual ancillary mode (L) on a beam splitter of transmittance η, which models the inefficient avalanche photodiode detector in our consideration.

Both the interactions are Gaussian in their nature and can be represented by a sequence of transformations

$$V(\zeta, \eta) = [\mathbb{1} \oplus \mathbb{1} \oplus V(\eta)]\,[\mathbb{1} \oplus V(\zeta) \oplus \mathbb{1}] \tag{V.32}$$

where the elements of the product are properly padded matrices (I.33) characterising the individual beam splitters and $\mathbb{1}$ represents a 2×2 identity matrix.

The Wigner function of the transformed state then reads

$$W'_{SAL}(\xi) = \sum_f \gamma_f K_{\mu'_f \Theta'_f}(\xi) \tag{V.33}$$

with the characteristic matrices and vectors of mean values transformed using the resulting matrix $V(\zeta, \eta)$ according to the relation (III.43).

(3) In the third part, the virtual ancillary mode (L) is traced out. The Wigner function $W'_{SAL}(\xi)$ is consequently transformed according to the relation (III.63)

$$W_{SA}(\xi) = \sum_f \gamma_f \frac{2\pi}{\det \lfloor \Theta'_f \rceil_L} K_{\mu'_f \Theta''_f}(\xi) = \sum_f \gamma''_f K_{\mu'_f \Theta''_f}(\xi) \tag{V.34}$$

where the cumulative factors γ''_f comprise

$$\gamma''_f = \gamma_f \frac{2\pi}{\det \lfloor \Theta'_f \rceil_L} \ . \tag{V.35}$$

(4) The Wigner function $W_{SA}(\xi)$ is transformed again in the detection process. Its transformation is governed by an equation similar to (III.65) in structure

with a different normalisation due to the number of signal modes

$$W^{\bigstar}(\xi_S) = (2\pi)^{-2} \frac{\sum_f \sum_{f'} \frac{\gamma''_f \gamma^{\bigstar}_{f'}}{\sqrt{\det \lfloor \Xi_{ff'} \rceil_A}} \exp\left(-\frac{1}{2}\zeta_{ff'}\right) K_{\delta_{ff'}\Xi'_{ff'}}(\xi_S)}{\sum_f \sum_{f'} \frac{\gamma''_f \gamma^{\bigstar}_{f'}}{\sqrt{\det \Xi_{ff'}}} \exp\left(-\frac{1}{2}\zeta_{ff'}\right)} \tag{V.36}$$

with the factors γ''_f coming from (V.35) and $\gamma^{\bigstar}_{f'}$ from (III.39).

The joint characteristic matrices Ξ_{ff}, the joint vectors of mean values $\delta_{ff'}$ and the additional factor $\exp\left(-\frac{1}{2}\zeta_{ff'}\right)$ are governed by the product relation (III.46), starting again with the individual matrices and vectors of (V.34) and (III.39). Furthermore the characteristic matrices $\Xi'_{ff'}$ result from the subsequent planar integral (III.57).

Finally the probability relation has to be scaled appropriately, reading

$$P^{\bigstar} = (2\pi)^4 \sum_f \sum_{f'} \frac{\gamma''_f \gamma^{\bigstar}_{f'}}{\sqrt{\det \Xi_{ff'}}} \exp\left(-\frac{1}{2}\zeta_{ff'}\right) \ . \tag{V.37}$$

In conclusion the only significant differences with the original relations (III.65) and (III.66) lie in the normalisation of the final expressions (V.36) for the Wigner function respective to detection outcome $\bigstar \in \{\circ, \bullet\}$ and the corresponding probability relation (V.37).

In the improved procedure introduced in the section II.2 we consider iterative chains where the signal state is recycled until the subtraction finally succeeds or a predetermined, reasonable number of attempts is eventually reached.

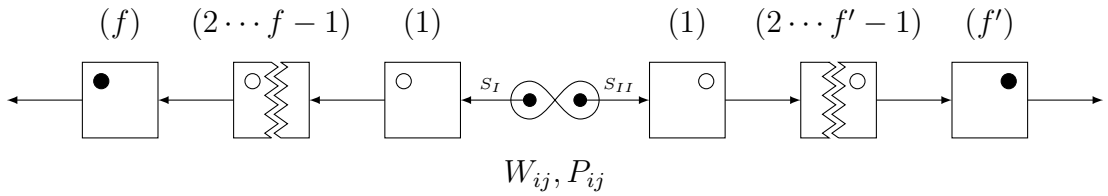

Figure V.3: The subtraction is repeatedly attempted on the first (S_I) arm of the entangled state until it succeeds in the fth step. Subsequently the subtraction process is repeated for the second (S_{II}) arm until it finally succeeds in the f'th step. The Wigner function of the resulting state is denoted $W_{ff'}(\xi_S)$ and the respective probability $P_{ff'}$.

Because the signal modes are entangled they can not be considered separately. The basic outline of the improved procedure adapted to reflect the entanglement of the signal mode is presented in the Figure V.3. In this iterative chain the subtraction finally succeeds in the fth attempt on the first mode (S_I) and in the f'th attempt on the second mode (S_{II}) of the entangled system. The conditional probability

$$\begin{aligned} P_{ff'} =& P_1^{\circ}(S_I)\cdots P_{f-1}^{\circ}(S_I)P_f^{\bullet}(S_I) \\ & P_1^{\circ}(S_{II})\cdots P_{f'-1}^{\circ}(S_{II})P_{f'}^{\bullet}(S_{II}) \end{aligned} \tag{V.38}$$

associated with the iterative chain represents the first $(f-1)$ failures followed by the final success on the first mode and similarly for the second mode where the success occurs after $(f'-1)$ failed attempts. The individual probabilities $P_f^{\bigstar}(\cdot)$ are given by the relation (V.37) with the symbols S_I and S_{II} distinguishing the interacting mode in the underlying subtraction procedure Figure V.2. The Wigner function respective to this chain is denoted $W_{ff'}(\xi_S)$.

The improved subtraction procedure either succeeds in any of the iterations under consideration or it fails completely. Because the first successful iteration is not known beforehand, we take all the possible iterative chains into account. Each of the iterative chains is statistically independent. The overall probability of successful subtraction is therefore obtained in the additive form

$$Q = \sum_{f}^{N}\sum_{f'}^{N} P_{ff'} \ , \tag{V.39}$$

where N represents the **maximal number of subtraction attempts on each**

mode of the signal. The overall Wigner function of the subtracted state

$$W\left(\xi_S\right) = Q^{-1} \sum_{f}^{N} \sum_{f'}^{N} P_{ff'} W_{ff'}(\xi_S) \tag{V.40}$$

describes the result of the modified distillation procedure [15] under our consideration. In line with the section V.1 and the distillation protocol itself we start with a signal two mode squeezed state which was briefly introduced in the subsection I.7.F. The state is Gaussian and its decomposition into Gaussian kernels is straightforward

$$W_S(\xi_S) = \gamma_1^S K_{\Theta_1^S}(\xi_S) \tag{V.41}$$

with the characteristic matrix Θ_1^S obtained as an inverse of the variance (I.52)

$$\Theta_1^S = 2 \begin{pmatrix} \cosh 2\gamma & \cdot & -\sinh 2\gamma & \cdot \\ \cdot & \cosh 2\gamma & \cdot & \sinh 2\gamma \\ -\sinh 2\gamma & \cdot & \cosh 2\gamma & \cdot \\ \cdot & \sinh 2\gamma & \cdot & \cosh 2\gamma \end{pmatrix} , \tag{V.42}$$

the vector of mean values $\mu_1^S \equiv 0$ and the normalisation (weight) factor given as

$$\gamma_1^S = \frac{\sqrt{\det \Theta_1^S}}{(2\pi)^2} = \pi^{-2} . \tag{V.43}$$

3 Probability and performance assessment

In our analysis of the distillation protocol we compare the effects of the improved subtraction procedure with the results obtained for the ideal subtraction. The performance of the distillation is assessed using the Gaussian logarithmic negativity and the EPR correlations introduced earlier in the section I.6.

The effects of the improved subtraction procedure for different **maximal numbers of subtraction attempts** N are presented in the Figure V.4 and the Figure V.5, where the mappings of the logarithmic negativities Λ and EPR correlations Υ are shown as functions of the overall success probability (V.39). Both the entanglement measures are functions of second moments of the quadrature operators of the distilled

states. In the case of the ideal subtraction the variance matrix is defined by the relation (V.27). In the case of the improved subtraction procedure the overall Wigner function (V.40) is simply decomposed into a linear combination of Gaussian kernels and the overall variance matrix can be straightforwardly extracted with the formula (B.6) derived in the appendix B.

The entanglement measures are computed numerically for an initial two mode squeezed vacuum state (I.52) with the squeezing rate $\gamma \equiv 1.00$. The numerical simulation is performed for both the ideal ($\eta = 1.00$) and the inefficient ($\eta = 0.64$) detection models.

The effects of the improved subtraction procedure measured in terms of the logarithmic negativity Λ are shown in the Figure V.4. We can see that the success probability Q can be improved by an order of magnitude by taking as little as 10 subtraction attempts into account. The probability can be further improved by increasing the number of attempts, however, the difference is not as significant. We can also see the distillation procedure is not negatively impacted by inefficient detection in terms of achievable logarithmic negativity. The inefficient detection only impacts the success rate of the distillation and decreases the improvements otherwise attainable by the improved procedure.

The Figure V.5 represents the effects measured in terms of the EPR correlations Υ. Similarly to the previous case we can see that the success probability Q can be improved by an order of magnitude by taking as little as 10 subtraction attempts. Likewise the inefficient detection does not negatively impact the attainable EPR correlations.

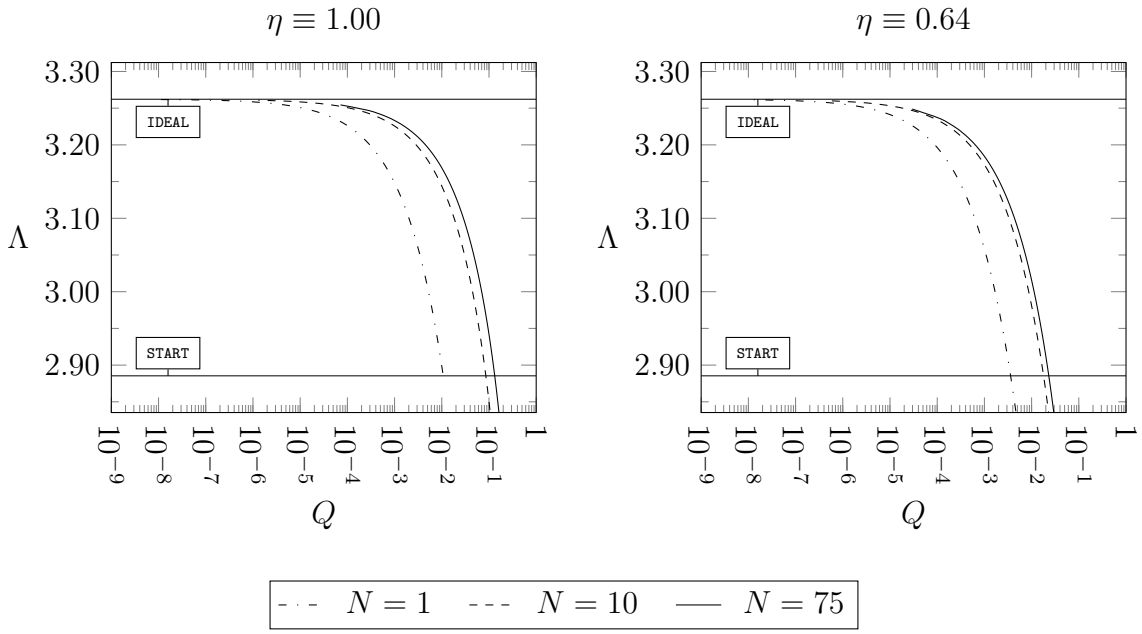

Figure V.4: The success probability Q can be improved by roughly on order of magnitude by taking as little as ten subtraction attempts in both the ideal (left plot) and realistic (right plot) detection models.

We show the mapping of Gaussian logarithmic negativity Λ for $N = 1$, $N = 10$, and $N = 75$ for detection efficiencies $\eta = 1.00$ and $\eta = 0.64$.

Furthermore we can see in the far right region of each plot that the procedure may succeed with negativity lower than it was in the beginning, effectively failing to distil any entanglement.

The horizontal `START` line indicates the logarithmic negativity of the initial state. The `IDEAL` line indicates the negativity of the state obtained with the ideal distillation procedure, giving an upper boundary on the performance of improved subtraction procedure.

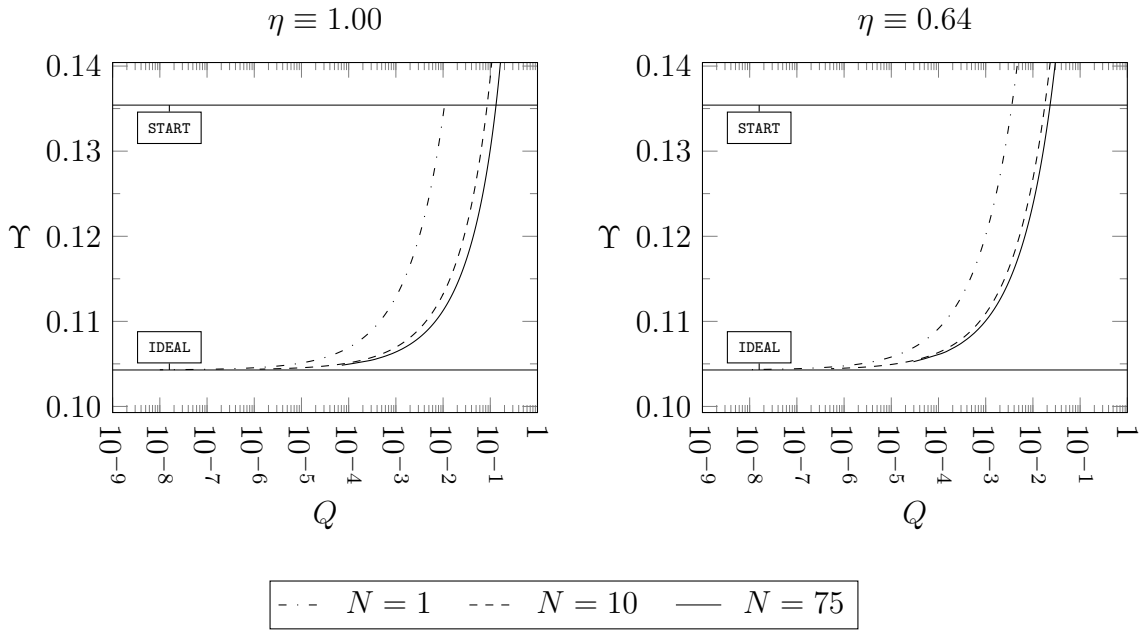

Figure V.5: The success probability Q can be improved by roughly on order of magnitude by taking as little as ten subtraction attempts in both the ideal (left plot) and realistic (right plot) detection models.

We show the mapping of EPR correlations Υ for $N = 1$, $N = 10$, and $N = 75$ for detection efficiencies $\eta = 1.00$ and $\eta = 0.64$.

Furthermore we can see in the far right region of each plot that the procedure may succeed with negativity lower than it was in the beginning, effectively failing to distil any entanglement.

The horizontal `START` line indicates the EPR correlations of the initial state. The `IDEAL` line indicates the correlations of the state obtained with the ideal distillation procedure, giving an upper boundary on the performance of improved subtraction procedure.

Conclusions and outlooks

We have introduced an improved single photon subtraction procedure and developed a mathematical description suitable for numerical simulations. We focused on two applications of the procedure; first we explored the preservation of quantum superposition by exploiting the properties of superposed coherent states and determined the preservation of quantum superposition to be considerably hindered by inefficient detection. In the case of ideal detection the procedure indeed preserved quantum superpositions with a high rate of success.

The second application involved quantum entanglement distillation. We compared the performance of the improved procedure for different maximal number of subtraction attempts. We observed an improvement of roughly one order of magnitude in success probability in comparison with the original, single step subtraction protocol. Unlike in the first application the inefficient detection was not fatal in respect to the attainable increase of entanglement and the only negative effect was a slightly lower success rate of the distillation procedure.

Further extensions to the work may include optimization of the procedure in terms of optimal parameters (primary beam splitter transmittance rate) under constraints imposed on the number of subtraction attempts and intensity of the signal mode. Furthermore the procedure could be extended to include additional losses and noise mixed into the signal mode in each subtraction attempt. In our current consideration the parameters of the improved procedure remain fixed for each subtraction attempt. A particularly interesting extension could be to adaptively change these parameters and search for their optimal values.

Moreover the current mathematical description supports a broader class of conditional operations comprising any number of ancillary modes and interactions characterised by Gaussian operations and measurements on avalanche photodiode de-

tectors. This makes, for example, description of a single photon addition quite straightforward task.

Furthermore our methodology may be used to model any quantum optical network consisting of linear optics, squeezing, and avalanche photodiode detectors, which essentially encompasses all existing quantum optical experiments. This ultimate goal would require a more robust, faster and scaleable implementation of the underlying numerical simulations.

Appendix A

Closed-form formulae of select series

In the chapter V we relied on closed-form formulae of a number of series. In this appendix we provide a step by step derivation of their final expressions.

Suppose $|\lambda| < 1$. Then the following series converge and their respective sums may be obtained as closed-form formulae

$$\sum_f \lambda^f = \frac{1}{1-\lambda} , \tag{A.1}$$

$$\sum_f \lambda^f f = \frac{\lambda}{(1-\lambda)^2} , \tag{A.2}$$

$$\sum_f \lambda^f f^2 = \frac{\lambda(1+\lambda)}{(1-\lambda)^3} , \tag{A.3}$$

$$\sum_f \lambda^f f^3 = \frac{\lambda(1+4\lambda+\lambda^2)}{(1-\lambda)^4} . \tag{A.4}$$

We are going to derive the formulae in the following paragraphs. We may recognize the geometric series (A.1) which converges for $|\lambda| < 1$ and the sum reads

$$S(0) = \sum_f \lambda^f = \frac{1}{1-\lambda} . \tag{A.5}$$

We may employ a simple trick to obtain the closed-form expressions for the rest of the series. Consider the derivative of a single element of the geometric series

$$\frac{\partial}{\partial\lambda}\lambda^f = f\lambda^{f-1} \tag{A.6}$$

which may be multiplied by the common ratio λ to yield

$$\lambda\frac{\partial}{\partial\lambda}\lambda^f = f\lambda^f \ . \tag{A.7}$$

The second series (A.1) may be rewritten with the aid of this relation into

$$\sum_f \lambda^f f = \lambda\frac{\partial}{\partial\lambda}\sum_f \lambda^f = \lambda\frac{\partial}{\partial\lambda}S(0) = \lambda S(1) \ , \tag{A.8}$$

where the symbol $S(f)$ denotes the fth derivative of the geometric series expression

$$S(f) = \frac{\partial^f S}{\partial\lambda^f} = \frac{f!}{(1-\lambda)^{f+1}} \ . \tag{A.9}$$

Higher orders of f in the series lead to a general closed-form expression

$$\sum_f \lambda^f f^\chi = \left(\lambda\frac{\partial}{\partial\lambda}\right)^\chi S(0) \ . \tag{A.10}$$

Consequently we may rewrite the series (A.3) and (A.4) into the following forms

$$\sum_f \lambda^f f^2 = \left(\lambda\frac{\partial}{\partial\lambda}\right)^2 S(0) = \lambda S(1) + \lambda^2 S(2) \ , \tag{A.11}$$

$$\sum_f \lambda^f f^3 = \left(\lambda\frac{\partial}{\partial\lambda}\right)^3 S(0) = \lambda S(1) + 3\lambda^2 S(2) + \lambda^3 S(3) \ . \tag{A.12}$$

The closed-form formulae of (A.2), (A.3), and (A.4) then clearly read

$$\sum_f \lambda^f f^1 = \lambda S(1) = \frac{\lambda}{(1-\lambda)^2} \,, \tag{A.13}$$

$$\sum_f \lambda^f f^2 = \lambda S(1) + \lambda^2 S(2) = \frac{\lambda}{(1-\lambda)^2} + \frac{2\lambda^2}{(1-\lambda)^3} = \frac{\lambda(1+\lambda)}{(1-\lambda)^3} \,, \tag{A.14}$$

$$\begin{aligned} \sum_f \lambda^f f^3 &= \lambda S(1) + 3\lambda^2 S(2) + \lambda^3 S(3) \\ &= \frac{\lambda}{(1-\lambda)^2} + \frac{6\lambda^2}{(1-\lambda)^3} + \frac{6\lambda^3}{(1-\lambda)^4} \\ &= \frac{\lambda(1+4\lambda+\lambda^2)}{(1-\lambda)^4} \,. \end{aligned} \tag{A.15}$$

Appendix B

Statistical moments of quadrature operators

The first two statistical moments of quadrature operators play an important role in a wide range of cases, including entanglement quantification (*cf.* section I.6).

A great advantage of Gaussian states is that the first two moments are well known as they completely characterise such states. The states in our consideration, however, decompose into linear combinations of Gaussian kernels (*cf.* chapter III) which makes the extraction of the first two moments a slightly more involved process.

We have shown that for every Gaussian function there exists a Gaussian kernel as its characteristic matrix is regular. Each decomposition (III.58) of a **physical state** may be equivalently represented by a linear combination of Gaussian functions

$$\begin{aligned} W(\xi) &= \sum_f \gamma_f \, K_{\mu_f \Theta_f}(\xi) \\ &= \sum_f \gamma_f \, \frac{(2\pi)^\chi}{\sqrt{\det \Theta_f}} \, G_{\mu_f \Theta_f^{-1}}(\xi) \\ &= \sum_f \beta_f \, G_{\mu_f \sigma_f}(\xi) \end{aligned} \tag{B.1}$$

with the weight factors β_f including the normalisation factors

$$\beta_f = \gamma_f \, \frac{(2\pi)^\chi}{\sqrt{\det \Theta_f}} \tag{B.2}$$

following from the correspondence between Gaussian kernels and Gaussian functions

$$G_{\mu\sigma}(\xi) = \frac{1}{(2\pi)^\chi \sqrt{\det \sigma}} \, K_{\mu\sigma^{-1}}(\xi) \; . \tag{B.3}$$

Ultimately we are interested in the expectation values $\langle \hat{\xi}_i \rangle$ and $\langle \hat{\xi}_i \hat{\xi}_j \rangle$ in respect to states described with the (B.1) distribution. These expectation values comprise the variance matrix and the vector of mean values.

Our knowledge is, however, limited to the individual vectors of mean values μ_f and variance matrices σ_f in respect to the individual Gaussian functions in the decomposition (B.1).

We start with the linear expectation values of the phase space variables

$$\begin{aligned}
\langle \hat{\xi}_i \rangle &= \iint \cdots \iint \xi_i \sum_f \beta_f \, G_{\mu_f \sigma_f}(\xi) \; \mathrm{d}^{2\chi}\xi \\
&= \sum_f \beta_f \iint \cdots \iint \xi_i \, G_{\mu_f \sigma_f}(\xi) \; \mathrm{d}^{2\chi}\xi \\
&= \sum_f \beta_f \langle \xi_i \rangle_f \\
&= \sum_f \beta_f (\mu_f)_i
\end{aligned} \tag{B.4}$$

where the operator $\langle \cdot \rangle_f$ denotes the expectation value in respect to the $G_{\mu_f \sigma_f}(\xi)$ and the symbol $(\mu_f)_i$ represents the ith element of the vector μ_f. The quadratic

expectation values read

$$\begin{aligned}
\langle\hat{\xi}_i\hat{\xi}_j\rangle &= \iint\cdots\iint \xi_i\xi_j \sum_f \beta_f\, G_{\mu_f\sigma_f}(\xi)\ \mathrm{d}^{2\chi}\xi \\
&= \sum_f \beta_f \iint\cdots\iint \xi_i\xi_j\, G_{\mu_f\sigma_f}(\xi)\ \mathrm{d}^{2\chi}\xi \\
&= \sum_f \beta_f \langle\xi_i\xi_j\rangle_f \\
&= \sum_f \beta_f \Big(\langle\xi_i\xi_j\rangle_f \pm \langle\xi_i\rangle_f\langle\xi_j\rangle_f\Big) \\
&= \sum_f \beta_f (\sigma_f)_{ij} + \sum_f \beta_f (\mu_f)_i (\mu_f)_j
\end{aligned} \tag{B.5}$$

where $(\sigma_f)_{ij}$ yields the ijth element of the variance matrix σ_f. The total variance in respect to the Wigner function (B.1) may now be obtained without any extensive effort using only the statistical properties of individual Gaussian functions

$$\begin{aligned}
\mathrm{var}(\hat{\xi}_i,\hat{\xi}_j) &= \frac{1}{2}\langle\hat{\xi}_i\hat{\xi}_j + \hat{\xi}_j\hat{\xi}_i\rangle - \langle\hat{\xi}_i\rangle\langle\hat{\xi}_j\rangle \\
&= \langle\hat{\xi}_i\hat{\xi}_j\rangle - \langle\hat{\xi}_i\rangle\langle\hat{\xi}_j\rangle \\
&= \sum_f \beta_f (\sigma_f)_{ij} + \sum_f \beta_f (\mu_f)_i (\mu_f)_j - \sum_f \beta_f (\mu_f)_i \sum_f \beta_f (\mu_f)_j
\end{aligned} \tag{B.6}$$

where all the elements are immediately known from the expression (B.1).

Bibliography

[1] O'Brien, J. L., Furusawa, A., and Vučković, J. "Photonic quantum technologies". In: *Nature Photonics* 3.12 (2009), pp. 687–695. DOI: 10.1038/nphoton.2009.229.

[2] "Quantum evolution". In: *Nature Photonics* 3.12 (2009), pp. 669–669. DOI: 10.1038/nphoton.2009.219.

[3] Walls, D. F. *Quantum optics*. Berlin: Springer, 2008.

[4] Braunstein, S. L. and Loock, P. van. "Quantum information with continuous variables". In: *Rev. Mod. Phys.* 77 (2 2005), pp. 513–577. DOI: 10.1103/RevModPhys.77.513.

[5] Weedbrook, C., Pirandola, S., García-Patrón, R., Cerf, N. J., Ralph, T. C., Shapiro, J. H., and Lloyd, S. "Gaussian quantum information". In: *Reviews of Modern Physics* 84.2 (2012), pp. 621–669. DOI: 10.1103/revmodphys.84.621.

[6] Adesso, G., Ragy, S., and Lee, A. R. "Continuous Variable Quantum Information: Gaussian States and Beyond". In: *Open Systems & Information Dynamics* 21.01n02 (2014), p. 1440001. DOI: 10.1142/S1230161214400010.

[7] Lloyd, S. and Braunstein, S. L. "Quantum Computation over Continuous Variables". In: *Physical Review Letters* 82.8 (1999), pp. 1784–1787. DOI: 10.1103/physrevlett.82.1784.

[8] Eisert, J., Scheel, S., and Plenio, M. B. "Distilling Gaussian States with Gaussian Operations is Impossible". In: *Physical Review Letters* 89.13 (2002). DOI: 10.1103/physrevlett.89.137903.

[9] Fiurášek, J. "Gaussian Transformations and Distillation of Entangled Gaussian States". In: *Physical Review Letters* 89.13 (2002). DOI: 10.1103/physrevlett.89.137904.

[10] Giedke, G. and Cirac, J. I. "Characterization of Gaussian operations and distillation of Gaussian states". In: *Physical Review A* 66.3 (2002). DOI: 10.1103/physreva.66.032316.

[11] Yukawa, M., Miyata, K., Mizuta, T., Yonezawa, H., Marek, P., Filip, R., and Furusawa, A. "Generating superposition of up-to three photons for continuous variable quantum information processing". In: *Optics Express* 21.5 (2013), p. 5529. DOI: 10.1364/oe.21.005529.

[12] Zavatta, A., Viciani, S., and Bellini, M. "Quantum-to-Classical Transition with Single-Photon-Added Coherent States of Light". In: *Science* 306.5696 (2004), pp. 660–662. DOI: 10.1126/science.1103190.

[13] Wenger, J., Tualle-Brouri, R., and Grangier, P. "Non-Gaussian Statistics from Individual Pulses of Squeezed Light". In: *Physical Review Letters* 92.15 (2004). DOI: 10.1103/physrevlett.92.153601.

[14] Kim, M. S., Park, E., Knight, P. L., and Jeong, H. "Nonclassicality of a photon-subtracted Gaussian field". In: *Physical Review A* 71.4 (2005). DOI: 10.1103/physreva.71.043805.

[15] Opatrný, T., Kurizki, G., and Welsch, D.-G. "Improvement on teleportation of continuous variables by photon subtraction via conditional measurement". In: *Physical Review A* 61.3 (2000). DOI: 10.1103/physreva.61.032302.

[16] Ourjoumtsev, A., Dantan, A., Tualle-Brouri, R., and Grangier, P. "Increasing Entanglement between Gaussian States by Coherent Photon Subtraction". In: *Physical Review Letters* 98.3 (2007). DOI: 10.1103/physrevlett.98.030502.

[17] Takahashi, H., Neergaard-Nielsen, J. S., Takeuchi, M., Takeoka, M., Hayasaka, K., Furusawa, A., and Sasaki, M. "Entanglement distillation from Gaussian input states". In: *Nature Photonics* (2010). DOI: 10.1038/nphoton.2010.1.

[18] Kurochkin, Y., Prasad, A. S., and Lvovsky, A. I. "Distillation of The Two-Mode Squeezed State". In: *Physical Review Letters* 112.7 (2014). DOI: 10.1103/physrevlett.112.070402.

[19] Provazník, J. "Adaptive subtraction of single photon from a state of light". Thesis. Univerzita Palackého v Olomouci, Přírodovědecká fakulta, Olomouc, 2015.

[20] Nielsen, M. A. *Quantum computation and quantum information*. Cambridge, U.K. New York: Cambridge University Press, 2000.

[21] Wang, X.-B., Hiroshima, T., Tomita, A., and Hayashi, M. "Quantum information with Gaussian states". In: *Physics Reports* 448 (1–4 2007), pp. 1–111. DOI: http://dx.doi.org/10.1016/j.physrep.2007.04.005.

[22] Leonhardt, U. *Measuring the Quantum State of Light*. Cambridge Studies in Modern Optics. Cambridge University Press, 1997.

[23] Greiner, W. *Quantum Mechanics : Special Chapters*. Berlin, Heidelberg: Springer Berlin Heidelberg, 1998.

[24] Sakurai, J. J. *Modern quantum mechanics*. Harlow, Essex: Pearson, 2014.

[25] Einstein, A., Podolsky, B., and Rosen, N. "Can Quantum-Mechanical Description of Physical Reality Be Considered Complete?" In: *Phys. Rev.* 47 (10 1935), pp. 777–780. DOI: 10.1103/PhysRev.47.777.

[26] Peres, A. "Separability Criterion for Density Matrices". In: *Physical Review Letters* 77.8 (1996), pp. 1413–1415. DOI: 10.1103/physrevlett.77.1413.

[27] Adesso, G. and Illuminati, F. "Entanglement in continuous-variable systems: recent advances and current perspectives". In: *Journal of Physics A: Mathematical and Theoretical* 40.28 (2007), pp. 7821–7880. DOI: 10.1088/1751-8113/40/28/s01.

[28] Simon, R. "Peres-Horodecki Separability Criterion for Continuous Variable Systems". In: *Physical Review Letters* 84.12 (2000), pp. 2726–2729. DOI: 10.1103/physrevlett.84.2726.

[29] Dodonov, V., Malkin, I., and Man'ko, V. "Even and odd coherent states and excitations of a singular oscillator". In: *Physica* 72.3 (1974), pp. 597–615. DOI: 10.1016/0031-8914(74)90215-8.

[30] Ford, G. and O'Connell, R. "Wigner Distribution Function Analysis of a Schrödinger Cat Superposition of Displaced Equilibrium Coherent States". In: *Acta Physica Hungarica B) Quantum Electronics* 20.1-2 (2004), pp. 91–94. DOI: 10.1556/aph.20.2004.1-2.17.

[31] Bennett, C. H. "Quantum Information". In: *Physica Scripta* T76.1 (1998), p. 210. DOI: 10.1238/physica.topical.076a00210.

[32] Gisin, N., Ribordy, G., Tittel, W., and Zbinden, H. "Quantum cryptography". In: *Rev. Mod. Phys.* 74 (1 2002), pp. 145–195. DOI: 10.1103/RevModPhys.74.145.

[33] Yu, T. and Eberly, J. H. "Sudden Death of Entanglement". In: *Science* 323.5914 (2009), pp. 598–601. DOI: 10.1126/science.1167343.

[34] Almeida, M. P., Melo, F. de, Hor-Meyll, M., Salles, A., Walborn, S. P., Ribeiro, P. H. S., and Davidovich, L. "Environment-Induced Sudden Death of Entanglement". In: *Science* 316.5824 (2007), pp. 579–582. DOI: 10.1126/science.1139892.

[35] Serafini, A., Paris, M. G. A., Illuminati, F., and Siena, S. D. "Quantifying decoherence in continuous variable systems". In: *Journal of Optics B: Quantum and Semiclassical Optics* 7.4 (2005), R19–R36. DOI: 10.1088/1464-4266/7/4/r01.

[36] Barbosa, F. A. S., Coelho, A. S., Faria, A. J. de, Cassemiro, K. N., Villar, A. S., Nussenzveig, P., and Martinelli, M. "Robustness of bipartite Gaussian entangled beams propagating in lossy channels". In: *Nature Photonics* 4.12 (2010), pp. 858–861. DOI: 10.1038/nphoton.2010.222.

[37] Bennett, C. H., Brassard, G., Popescu, S., Schumacher, B., Smolin, J. A., and Wootters, W. K. "Purification of Noisy Entanglement and Faithful Teleportation via Noisy Channels". In: *Physical Review Letters* 76.5 (1996), pp. 722–725. DOI: 10.1103/physrevlett.76.722.

[38] Furusawa, A. "Unconditional Quantum Teleportation". In: *Science* 282.5389 (1998), pp. 706–709. DOI: 10.1126/science.282.5389.706.

[39] Braunstein, S. L. and Kimble, H. J. "Teleportation of Continuous Quantum Variables". In: *Physical Review Letters* 80.4 (1998), pp. 869–872. DOI: 10.1103/physrevlett.80.869.

[40] Ralph, T. C. "Continuous variable quantum cryptography". In: *Physical Review A* 61.1 (1999). DOI: 10.1103/physreva.61.010303.

[41] Su, X., Wang, W., Wang, Y., Jia, X., Xie, C., and Peng, K. "Continuous variable quantum key distribution based on optical entangled states without signal modulation". In: *EPL (Europhysics Letters)* 87.2 (2009), p. 20005. DOI: 10.1209/0295-5075/87/20005.

[42] Madsen, L. S., Usenko, V. C., Lassen, M., Filip, R., and Andersen, U. L. "Continuous variable quantum key distribution with modulated entangled states". In: *Nature Communications* 3 (2012), p. 1083. DOI: 10.1038/ncomms2097.